Metamorphic rocks in a section across a Svecnorwegian eclogite-bearing deformation zone in Halland: characteristics and regional context

Brendan Dyck

Bachelor thesis in geology at Lund University - Lithosphere and Paleobiosphere Sciences, no. 269 (15 hskp/ECTS)

Department of Earth- and Ecosystem Sciences
Division of Geology
Lund University
2010

Metamorphic rocks in a section across a Sveconorwegian eclogite-bearing deformation zone in Halland: characteristics and regional context.

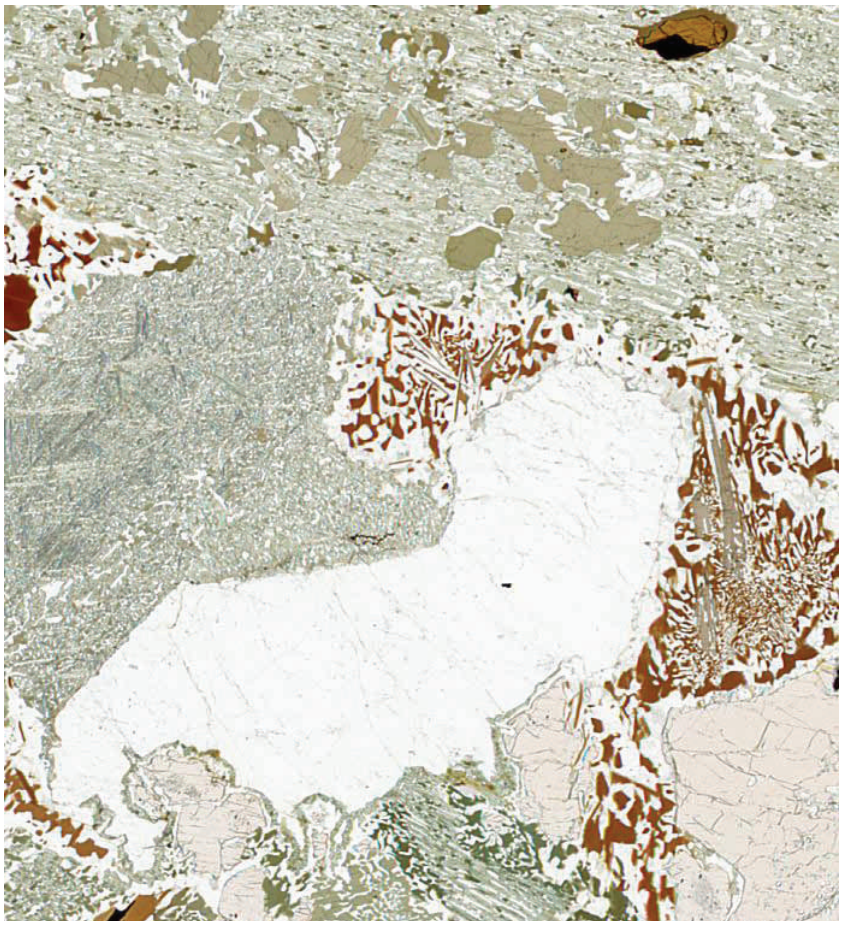

Examensarbete

Brendan Dyck

Department of Geology
Lund University
2010

Contents

Cover Picture: Scanned thin section from a retrogressed eclogite showing pseudomorphs of large grains, mineral relations and textures. Figure 16 in text.

Metamorphic rocks in a section across a Svecnorwegian eclogite-bearing deformation zone in Halland: characteristics and regional context

BRENDAN DYCK

Dyck, B., 2010: Metamorphic rocks in a section across a Sveconorwegian eclogite-bearing deformation zone in Halland: characteristics and regional context. *Examensarbeten i geologi vid Lunds universitet*, Nr. XX, 23 pp. (15 ECTS credits).

Abstract:

Eclogitized mafic bodies in the Ullared Deformation Zone (UDZ) of SW Sweden are evidence for high-pressure metamorphism and deformation related to continent collision during the Sceconorwegian orogeny. A petrographic study was performed on ten samples taken from a profile transecting the UDZ, with the aim of further characterizing the rocks within the eclogite bearing deformation zone. The UDZ is compositionally heterogeneous, containing felsic to intermediate gneisses and augen gneisses, which host bodies of mafic rocks. Samples of felsic gneisses, garnet amphibolites and one retrogressed eclogite were studied. Quartz, plagioclase, microcline, biotite and hornblende were the main minerals present in the felsic rocks. The amphibolites were predominately composed of hornblende, garnet, plagioclase and clinopyroxene. Crystal recovery in the form of recrystallization and annealing occurred in the strongly deformed gneisses. Due to a competency contrast at higher temperatures, the signs of high-strain are more common in the felsic rocks than in the amphibolites. In the retro-eclogite, clinopyrozene+plagioclase+hornblende and biotite+plagioclase symplectites are thought to have formed from the decomposition of omphacite and phengite respectively. Scapolite was found in five of the ten samples, both mafic and felsic, suggesting that chlorine and CO_2 rich fluids infiltrated the rocks during metamorphism. Parts of the UDZ have been strongly deformed and mylonitized under high-pressure granulite to upper-amphibolite facies Sveconorwegian metamorphism. The eclogites have been interpreted as *in situ* in relation to the surrounding UDZ gneisses, meaning they were not formed at higher pressures than what the rest of the UDZ was subjected to, and they were not tectonically emplaced. The upper-amphibolite conditions are thought to have overprinted higher pressure assemblages with variable efficiency leaving remnant eclogite textures in some less affected mafic bodies.

Keywords: Eclogite, Sveconorwegian, high-grade metamorphism, retrogression, Ullared Deformation Zone.

Brendan Dyck, Department of Earth & Ecosystem Sciences, Lund University, Sölvegatan 12, SE-223 62 Lund, Sweden. E-mail: brendan.dyck@gmail.com

1 Introduction

1.1 Background

The Sveconorwegian orogen of southwest Sweden and Norway is characterized by metamorphosed Precambrian crustal and supracrustal rocks which occur both as autochthonous segments and allochthonous terranes. It is recognized as part of the Grenvillian orogenic belt and has tectonic counterparts around the world, including Canada and Scotland (e.g., Johansson et al, 2001). A simplistic model of the Sveconorwegian orogenic belt divides the belt into five sections; the Telemarkia terrane, the Bamble terrane, the Kongsborg terrane, the Idefjorden terrane and the Eastern Segment (Bingen et al. 2008; Fig. 1). Metamorphic conditions varied across the Eastern Segment: the northern portion underwent greenschist and amphibolite facies metamorphism, whereas the southern reached higher temperatures and pressures, up to high-pressure granulite facies (Möller 1999; Söderlund et al, 2004). The southern portion of the Eastern Segment is predominantely composed of upper amphibolite and high-pressure granulite facies orthogneisses and metabasic rocks. Eclogite remnants occur in the Ullared Deformation Zone (UDZ), a zone characterized by strongly deformed to mylonitic gneisses. U-Pb dating of zircon inclusions in kyanite and garnet in eclogite from the UDZ has yielded a maximum age of 972 ± 14 Ma for the eclogitization (Johansson et al, 2001). Following the eclogitization there was rapid exhumation of the eclogites and surrounding strongly-deformed rocks. Parts of this exhumation have been interpreted to have taken place during general relaxation and gravitational collapse of the orogenic belt (e.g. Bingen et al. 2008, Möller et al. 2007). Remaining tectonic questions include the tectonic significance of the Ullared Deformation Zone and the mechanism for exhumation of the eclogites.

The present study is comprised of 1) a literature review on the regional geology, 2) a petrographic description of ten samples from across the Ullared Deformation Zone, and 3) a discussion on how the metamorphic assemblages and textures in the studied samples relate to the regional context.

1.2 Methods

The samples were collected during 2009 by Charlotte Möller as a part of a 25 km long N-S profile, from Sjönevad in the south to Lia in the north, in connection with the initiation of a bedrock mapping project "Falkenberg" by the Geological Survey of Sweden. The samples and thin sections were provided by Jenny Andersson at the Geological Survey of Sweden. The location of the samples is marked on figure 2. The focus of the thin section study was petrography and metamorphic textures. Of the ten sections, two were selected for further studies using a Scanning Electron Microscope (SEM) available at Lund University's Geocentrum. Results and photos are taken with the SEM backscatter electron detector. The machine was not optimized for quantitative analysis, so precise chemistry was not studied. The results of the optical microscopy and SEM study were then interpreted in a regional context, and related to previous studies.

2 Regional Review

The remnant Sveconorwegian orogenic belt is a 500 km wide zone in the southwest Baltic Shield composed predominantly of Proterozoic aged gneiss units. Geochronology results from a multitude of samples taken in the past forty years confines the Sveconorwegian orogen at 1140-900 Ma (Bingen et al, 2008). A cumulative probability curve of all published Sveconorwegian age results complied by (Bingen et al, 2008) show two age peaks for metamorphism, one around 1035 Ma and the other around 930 Ma. The latter age is likely a result of a gravitational collapse that occurred when collisional forces weakened or ceased (Bingen et al, 2008). The now deeply eroded orogen is recognized as a tectonic extension to the Canadian Grenvillian orogenic belt and resulted from a collision between Baltica and at least one other major continent. One tectonic interpretation suggests Amazonia is the other colliding continent, but subsequent evidence is still lacking to confirm this theory (Hoffman, 1991). The orogen is confined in the east by the Sveconorwegian Frontal Deformation Zone (SFDZ) and in the west by Caledonian nappes (Wahlgren et al, 1994). Studies of the west are difficult since they must also deal with the deformation attributed to the younger Caledonian orogeny. Exposure varies greatly across the Sveconorwegian belt, but from what studies have been performed five distinct lithotectonic units are recognized (Bingen et al, 2005). These units are all N-S-trending and are separated by deeply rooted deformation zones (Park et al, 1991). The primary lithotectonic units from west to east are; the Telemarkia Terrane, the Kongsberg Terrane, the Bamble Terrane, the Idefjorden Terrane and the Eastern Segment. The Fennoscandia foreland of the Sveconorwegian belt is made up of Paleoproterozoic crust of the Svecofennian belt and the Transcandinavian Igneous Belt (TIB; Wahlgren et al, 1994).

2.1 The Four Phase Model

by Bingen et al, 2008

2.1.1 Arendal phase (1140-1080 Ma)

An eloquent model presented by (Bingen et al, 2008) separates the Sveconorwegian orogeny into four time-constricted phases. The first phase of the model is termed the Arendal phase, which occurred 1140-1080 Ma. Metamorphism of the Bamble and Kongsberg

terranes occurred during the early Arendal phase (1140-1125 Ma), and was likely caused by convergence of the Telemarkia and Idefjorden terranes (Andersson et al, 1996). When the Telemarkia and Idefjorden terranes came together in the late Arendal phase (1090-1080 Ma), the smaller Bamble and Kongsberg terranes were thrusted up to create an orogenic wedge. Intermediate pressure granulite facies metamorphism occurred throughout the orogenic wedge as a result of the crustal thickening during continent convergence (Bingen et al, 2008). Erosion of the uplifted terranes accompanied with nearby deposition of immature clastic sediments deposited after 1120 Ma are evidence for the development of foreland basin related to mountain building (de Haas et al, 1999).

2.1.2 Agder phase (1050-980 Ma)

The Agder phase is considered the main orogenic event that occurred in the Sveconorwegian orogen, which resulted in magmatism, metamorphism and mountain building (Bingen et al, 2008). At 1050 Ma as a result of a collision with at least one major continent, possibly Amazonia, the Idefjorden Terrane was metamorphosed. (Hoffman, 1991; Söderlund et al, 2008). Metamorphism related to this stage varies from lower amphibolite faceis to high-pressure granulate facies. Metamorphism of the Idefjorden Terrane and concurrent magmatism and plutonic emplacement in the Telemarkia Terrane likely result from tectonic overloading and tectonic thickening (Bingen and van Breeman, 1998). Studies show that in the Rogaland-Vest Agder Sector of the Telemarkia Terrane, the metamorphism occurred for at least 100 million years between 1035 and 900 Ma as evidenced by various studies using a compilation of methods by means of zircon, titanite and molybdenite geochronology (Bingen et al, 2008).

2.1.3 Falkenberg phase (980-970 Ma)

Metamorphism of the Eastern Segment took place during the Falkenberg and Dalane phases, this paper focuses primarily on events, which occurred in this time period. Eclogite relicts in the Eastern Segment provide evidence for deep, at least 50 km, burial of crustal units followed by rapid exhumation to mid crustal levels (Möller et al, 1998; 1999). Amphibolization and migmatization in the Mylonite Zone are evidence for juxtaposition of the Idefjorden Terrane the high-grade segment (Andersson et al, 2002). One possible interpretation is that the Falkenberg phase is a transition between compression and extension, and represents an end to the collisional forces responsible for the orogeny.

2.1.4 Dalane phase (970-900 Ma)

The Dalane phase is characterized by relaxation and gravitational collapse of the orogenic belt. In the Eastern segment this involved rapid exhumation of eclogites and surrounding high-grade rocks (Möller, 1998). Exhumation of the Eastern Segment was accomplished by displacement along the SFDZ and Protogine shear zone in the east and the Mylonite Zone in the west (Möller et al, 2007). In the southern part of the Telemarkia Terrane, exhumation of gneiss domes was accompanied by decompressive melting and monzodiorite-granite plutonism (Tomkins et al, 2005). Multiple units underwent high-temperature low-pressure metamorphism that is recognized as the final overprint from the Sveconorwegian orogeny (Bingen et al, 2008).

2.2 The Eastern Segment

During the Falkenberg phase of the Sveconorwegian orogeny the southern Eastern Segment was tectonically buried to depths in excess of 35 km. Some of the highest-grade metamorphism of the Sveconorwegian occurred and was recorded in units within the Eastern Segment (Johansson et al, 1991). The Eastern Segment is considered a parautochthonous unit equal in composition and age to the Fennoscandian basement. The protolith to the majority of the Eastern Segment is 1730-1660 Ma granitoid and granite massifs with associated mafic intrusions, similar to the Transscandinavian Igneous Belt (Söderlund et al, 2002; Möller et al, 2007). Metamorphic conditions varied throughout the Eastern Segment. North of lake Vänern the metamorphic conditions ranged from greenschist to amphibolite, whereas in the south, upper-amphibolite to granulite conditions occurred (Möller 1999; Söderlund et al, 2004). Pressure temperature estimates for the southern part of the Eastern Segment fall in the range of 680-800°C and 8-12 kbar (Wang and Lindh, 1996). In the Southern areas remnant eclogite boudins indicate high-pressure conditions (>15kbar ; >50km). Large nearly upright E-W-trending folds with wavelengths ranging between 4-15 km are recognizable on aeromagnetic anomaly maps of the southern Eastern Segment (Möller et al, 2007). Due to the high-temperature metamorphism of the Sveconorwegian orogeny, nearly all minerals have re-equilibrated and/or recrystallized. This makes interpreting the Sveconorwegian versus pre-Sveconorwegian metamorphism challenging. Söderlund et al (2002) and Möller et al (2007) presented evidence from zircon U-Pb geochronology that shows regional scale migmatization dated between 1460 and 1420 Ma. This event is termed the Hallandian event. As concluded by Söderlund et al (2005) metamorphic zircon growth is controlled by the amount of unexhausted Zr-bearing phases, as a result the ages of secondary zircon may not always be the age of peak conditions. Following the Hallandian event, there were 1400-1380 Ma intrusions of granitic and syenitoid rocks with an associated charnockitisation of surrounding gneiss units (Andersson et al, 1999). The Eastern Segment has had a complicated polymetamorphic history, with varying grades of metamorphism migmatization and retrogression.

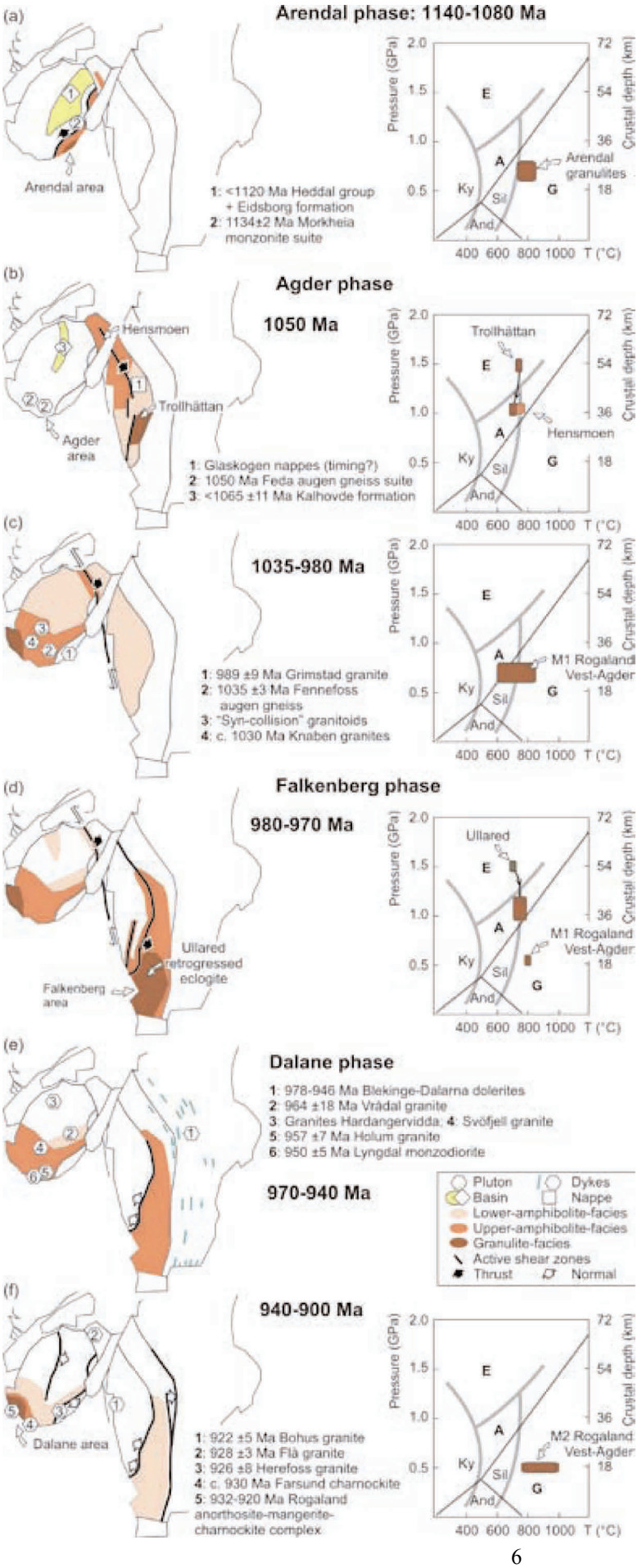

Figure 1. Sketched maps showing the location of metamorphism, magmatic rocks and sedimentary basins during the Sveconorwegian orogeny. (a) Arendal phase: 1140-1080 Ma. (b,c) Agder phase: 1050-980 Ma. (d) Falkenberg phase: 980-970 Ma. (e,f): Dalane phase: 970-900 Ma. Figure used with permission from Bernard Bingen.

Figure 2. Topographic map showing sample localities. © Sveriges Geologiska Undersökning, 2000.

2.3 The Ullared Deformation Zone

In the Eastern Segment there exists a several kilometer wide zone coined the Ullared Deformation Zone (UDZ). An outline of the UDZ can be recognized on high-resolution aeromagnetic maps, and eclogite and retrogressed eclogite localities from within the Eastern Segment are found within and above the UDZ (Johansson et al, 2001; Hegart, 2005). The UDZ runs southeast from the southern portion of the Mylonite Zone into the Eastern Segment. The zone is approximately 3-10 km wide and can be followed for at least 30km. Compositionally, the UDZ is heterogeneous and similar to other portions of the Eastern Segment, containing felsic to intermediate gneisses and augen gneisses with inset mafic units (Möller et al, 1997). Parts of the UDZ have been strongly deformed and mylonitized under high-pressure granulite to upper amphibolite facies Sveconorwegian metamorphism (Möller, 1999). Mafic lenses and units in the UDZ range in size from a few centimeters to several kilometers and are generally less deformed than the surrounding gneiss units. The UDZ is an important geological

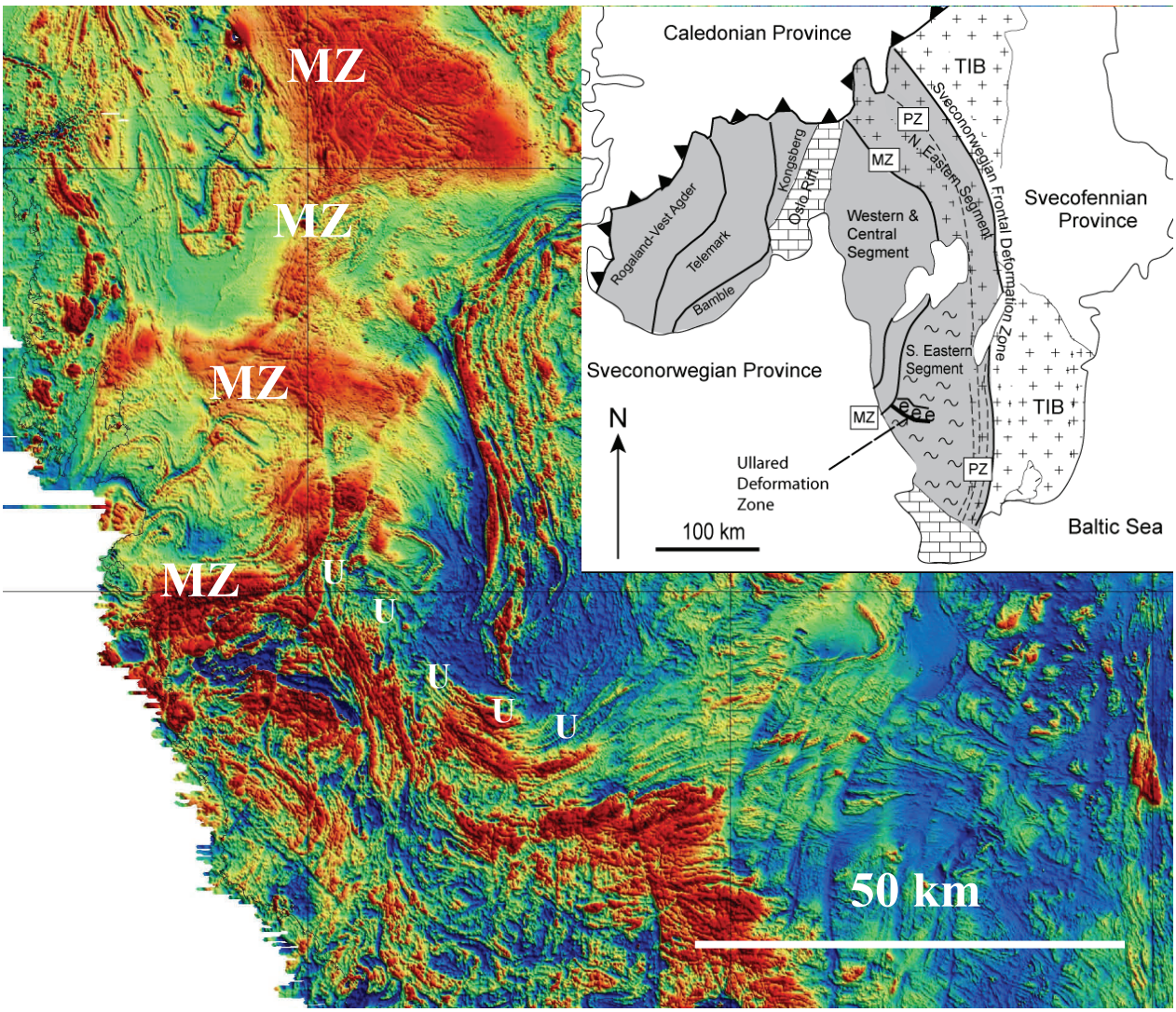

Figure 3. Magnetic anomaly map of part of the Eastern Segment. © Geological Survey of Sweden. MZ = Mylonite Zone, U = Ullared Deformation Zone. Inset: southwest Scandinavia showing the main lithotectonic units and shear zones of the Sveconorwegian orogen as well as the location of the nearby TIB units. (used with permission from Charlotte Möller)

unit for studying the Eastern Segment, because it represents the variety of conditions and the extreme pressures, which some parts of the Eastern Segment experienced during the Sveconorwegian orogeny. The maximum age of eclogitization subsequent and peak metamorphism as determined by Johansson et al (2001) using ion micropobe dating of zircon inclusions in garnets is 972 ± 14 Ma. The eclogized mafic lenses are structurally conformable with the surrounding gneiss units, so 972 ± 14 Ma can be interpreted as peak-pressure metamorphic age for the whole UDZ (Johansson et al, 2001). Eclogitization took place in the Falkenberg phase of the model proposed by Bingen et al (2008), but much of the deformation that happened in the UDZ took place during the Dalane phase, presumably in a sequence of eclogite emplacement followed by gravitational collapse and extension (Möller et al, 1997). Extension may result from thinning caused by gravitational spreading, tectonic unroofing and erosion. Erosion is unlikely the lone factor in the thinning which uplifted the rocks, because the time constraints, a few million years, are to short for erosion of more than 30 km at normal erosion rates. Tectonic stripping of the overburden is the most probable cause for the uplift of the eclogized units and high-pressure granulites to mid-crustal levels.

3 Sample Descriptions

3.1 CHM092003(A,B,C): Kilahed

3.1.1 Field Observations

Compositional layering of darker (more mafic) and lighter gneisses. Three gneiss units are distinguishable; one is recognizable by its light coloring. The difference between the two darker units is size and abun-

dance of garnet. Migmatization and recrystallization have produced a sugary granular texture. In the more felsic gneisses hand sample appears migmatized and large quartz domains are recognized. Gneissic banding is observable in hand section and outcrop scale (figure 4.). A penetrative foliation consistent in all units was measured at 300°/55° dipping NE.

Figure 4. Field photo from Kilahed location. Sharp contacts between migmatitic gneiss and garnet amphibolite. Photo taken by Charlotte Möller.

3.2 CHM092003A:Migmatitic amphibolite

3.2.1 Descriptions

This sample is a pyroxene bearing garnet-amphibolite. The mineral phases and textures are metamorphic, and there is a faint banding with microlayers richer in hornblende. Banding is only evident in low magnification due to the medium size of crystals. Main minerals present are; hornblende, plagioclase, clinopyroxene; garnet, biotite, quartz, microcline, scapolite are also present together with accessory apatite, pumpellyite, opaque and rounded metamorphic zircon. There is a fibrous intergrowth of biotite and a secondary mineral, probably pumpellyite (figure 7), and this intergrowth as well as all other elongate minerals align within ~35 degrees of parallel. Albite twinning in plagioclase is discordant and irregular. Pinning and dragging microstructures, as described by Passchier and Trouw (1996) occur in the plagioclase and quartz crystals.

3.2.2 Interpretations

Figure 5. Garnet amphibolite Photo taken by Charlotte Möller.

Figure 6. CHM092003A: Migmatitic amphibolites. Cropped segment from scanned thin section showing the assemblage and general texture.

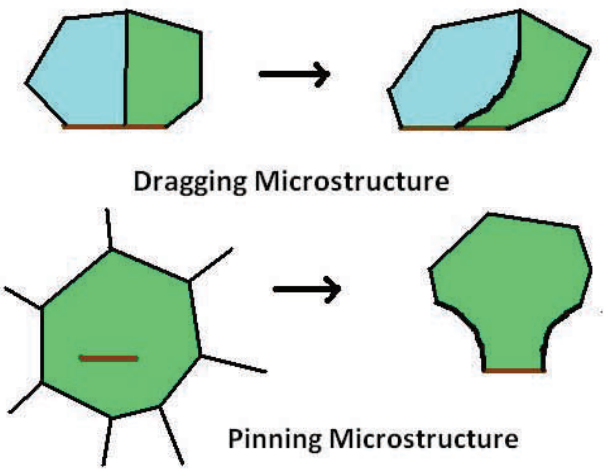

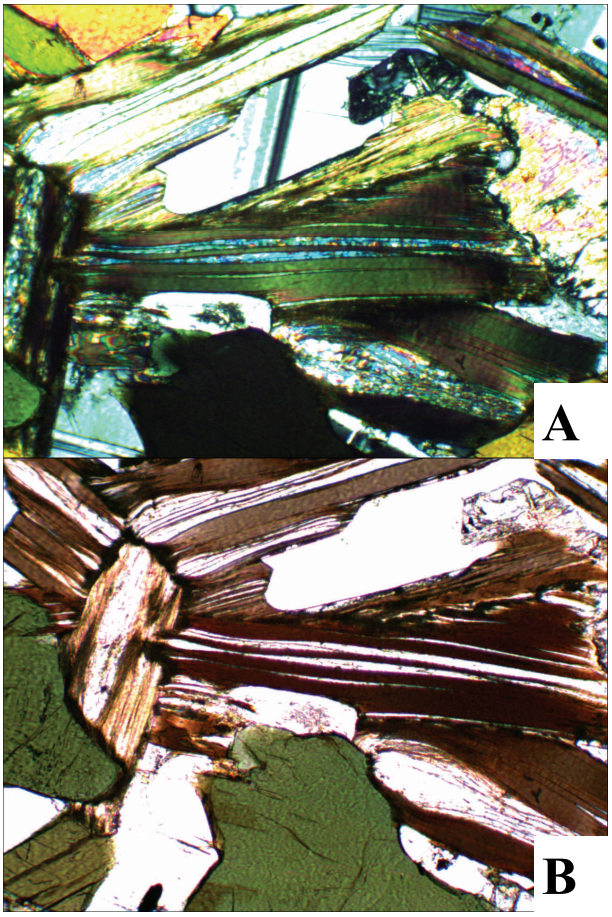

Figure 7 **A**) crossed polars photomicrograph of biotite (center) and pumpellyite intergrowth, large bottom center grain is hornblende, bright colored grain center right is scapolite **B**) plane polar view of the same grains.

This rock has undergone deformation under high temperature conditions. Dynamic recrystallization likely occurred in this rock, pinning and dragging microstructures in thin section and the sugary texture in hand sample evidence this. Garnet grains have collars of plagioclase, which suggests disequilibrium between garnet and hornblende or other phases, a reaction that has plagioclase as a product. The tapered twins and irregular albite twinning in plagioclase suggest a metamorphic origin. Based on textural relations, pyroxene and garnet are the only minerals that may have a previous origin stemming from different metamorphic conditions. The scapolite phase suggests a presence of CO_2 and Cl rich metamorphic fluids interacting with the rock. Triple junctions have been reached in some microdomains but the majority of crystals still show signs of stress. The most recent metamorphism was a low-grade event responsible for the local alteration of the quartz, plagioclase, and scapolite, possibly sericite, and also the pumpellyite alteration of biotite.

3.3 CHM092003B: Migmatized gneiss

3.3.1 Descriptions

This specimen is a migmatized gneiss with sparse garnet and hornblende. Quartz, microcline and plagioclase in near equal proportions account for 85 percent of this sample. Biotite flakes that are weakly aligned are scattered throughout this sample, forming aggregates in only a few areas. Hornblende is subhedral and only present in the few mafic domains. There is heterogeneity in grain sizes of the quartz and feldspars. The larger quartz crystals are elongate and trend the same as the biotite flakes. Grain boundaries in leucosomes are irregular. There are tapered twins in many of the plagioclase crystals. Minor amounts of scapolite occur with hornblende.

3.3.2 Interpretations

Quartz and feldspar grains in this sample show signs of stress and recovery. There are some large quartz crystals showing undulose extinction and some showing signs of subgrain amalgamation. The tapered twins in plagioclase point towards a metamorphic origin, but in comparison to sample 2003A the twinning process

Figure 8. Migmatitic gneiss , photo taken by Charlotte Möller

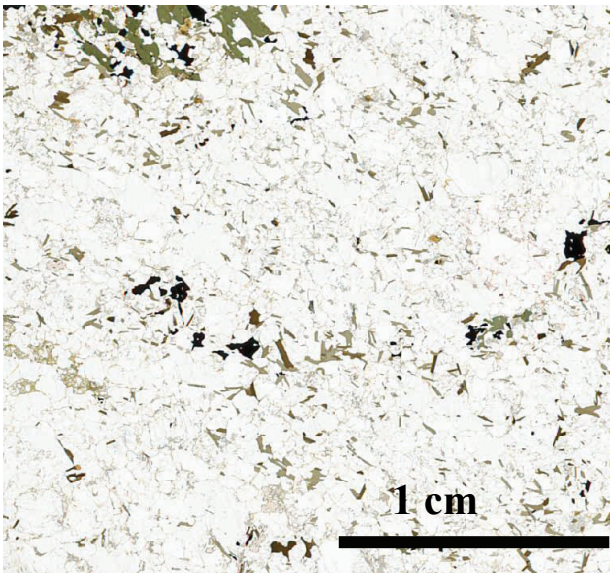

Figure 9. CHM092003B: Migmatized gneiss. Cropped segment from scanned thin section showing textures and crystal relations.

is nearer completion i.e. the tapered twins have developed into nearly planar textures. Scapolite indicates CO_2 and/or Cl rich fluid in the rock, due to its close proximity to 2003A it is expected to result from the same event. Minerals and textures in this section appear to have undergone a greater degree of recovery than those in 2003A as seen in the homogenous sizes of recrystallized quartz grains; this may be explained by the differences in rheology.

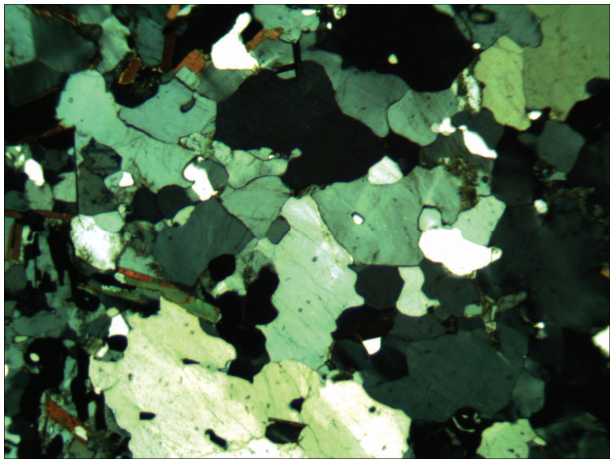

Figure 10. Photomicrograph of CHM092003B: Migmatized gneiss. Quartz grains partially recrystallized to large homogeneous grains. Note the formation of triple-junctions between recrystallized grains.

3.4 CHM092003C: Garnet amphibolite

3.4.1 Descriptions

This sample is a garnet amphibolite gneiss. Hornblende, plagioclase, garnet and biotite are the major minerals present in this section. Scapolite, quartz and clinopyroxene also exist but only as minor phases. A foliation is recognizable which has formed indistinct microdomains richer in plagioclase and quartz. The garnet crystals are subhedral and spotted with inclusions of plagioclase and biotite. Scapolite grains are

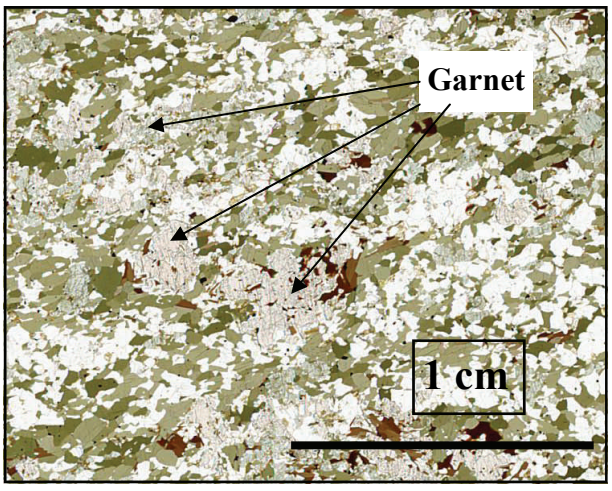

Figure 11. CHM92003C: Garnet amphibolite. Cropped segment from scanned thin section showing mineral assemblages and the general texture, note the size and amount of garnet.

euhedral, and have grown with all other phases. The plagioclase crystals exhibit tapered twins and show signs of strain.

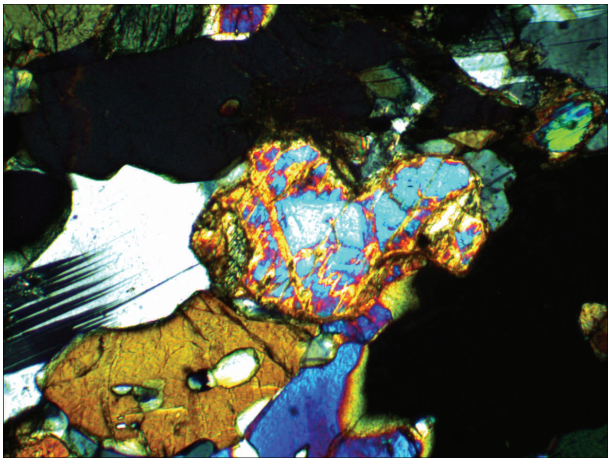

Figure 12. CHM092003C: Garnet amphibolite, crossed polars. Tapered twins in plagioclase and typical high birefringent scapolite grain.

3.4.2 SEM

Scapolite was analyzed and easily recognized by its sulfur peak, in this sample the scapolite has a ~2/1 ratio of Ca to Na.

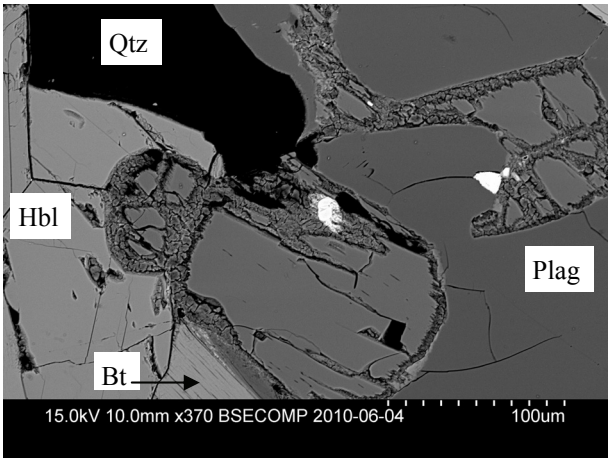

Figure 13. Scapolite grain (center), showing textural equilibrium between hornblende, scapolite, plagioclase, quartz and biotite, and late alteration of scapolite.

3.4.3 Interpretations

Compared to the other two units from this locality, this sample has the largest amounts garnet and is the least migmatitic. Hornblende and biotite appear to have formed later in this rocks metamorphic history, whereas the plagioclase, although metamorphic, probably formed earlier with the garnet and pyroxene. Scapolite looks to be confined by the growth of hornblende and biotite, which suggests these phases grew at the same time. Based on the Ca/Na ratio, the scapolite is composed of 2/3 meionite and 1/3 marialite. This section with the aid of 2003A and 2003B tell a polymetamorphic history that includes one medium-high-pressure event responsible for the formation of

garnet and pyroxene, and at least one lower pressure event responsible for the hornblende, biotite and scapolite formation. A deviatoric stress field existed for the lower pressure event, which has strained crystals and caused dynamic recrystallization to occur in the quartz and feldspar grains. A difference in the degree of foliation and recrystallization between the samples can be attributed to differences in composition and thereby rheology.

3.5 CHM092019A: Migmatized gneiss, Haxered

3.5.1 Descriptions

Quartz constitutes approximately 60 percent of this rock and when combined with the 30 percent that is plagioclase, this sample becomes quite felsic. Sparse small garnet crystals exist and appear broken and resorbed. Biotite makes up about 10 percent of the sample and appears as small euhedral grains some of which are altered to pumpellyite. Hornblende exists in very minor amounts, two grains detected, and looks mechanically fractured. Quartz occurs as well-formed elongate grains and in some cases as smaller grain aggregates, which exhibit the irregular grain boundaries associated with dynamic recrystallization. Plagioclase albite twins are well formed and parallel in nearly all grains. All phases except garnet look chemically stable, as no reaction zones are visible.

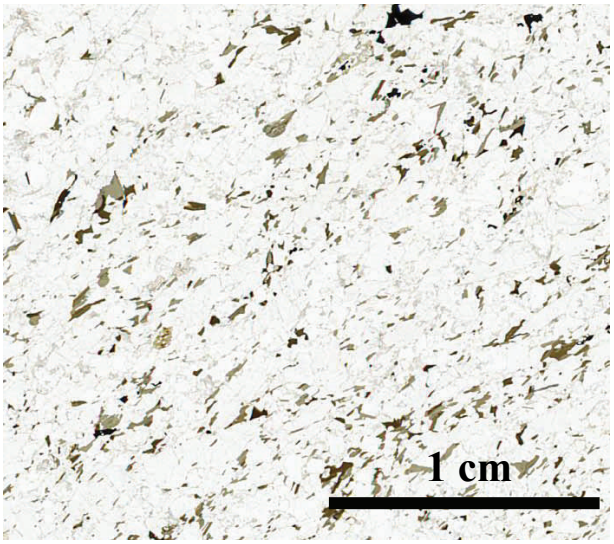

Figure 14. CHM092019A: Migmatized gneiss. Cropped segment from scanned thin section showing mineral assemblages and the general texture.

3.5.2 Interpretations

The metamorphic grade is upper amphibolites facies. High temperature deformation is responsible for the reformation of quartz to euhedral elongate grains, although this process did not go to completion as seen by the presence of quartz and plagioclase aggregates. The plagioclase probably recrystallized alongside the quartz, and the well-formed twins in most grains indicate plagioclase recrystallization is near completion. The garnets are resorbed, and the only phase that does not appear to be in equilibrium.

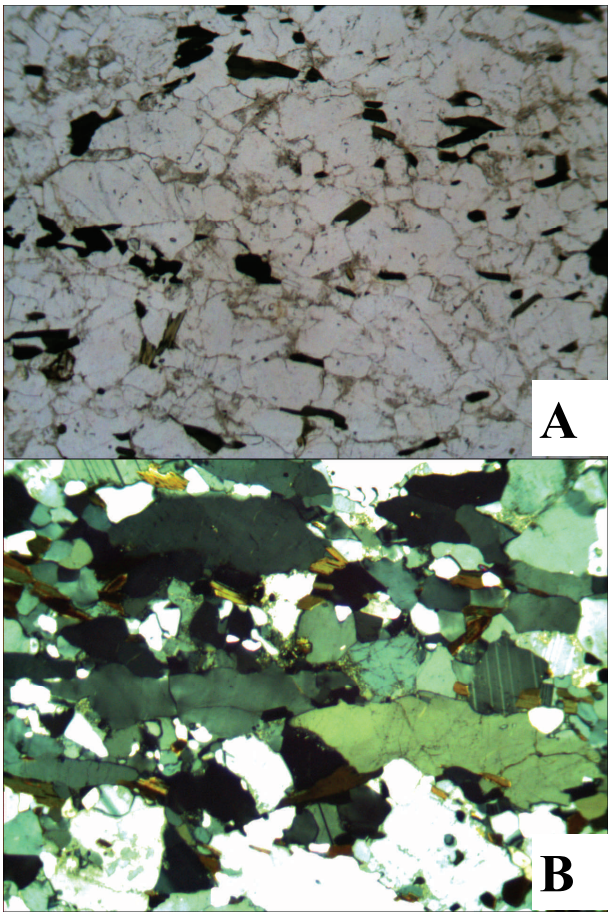

Figure 15. CHM092019A: Migmatized gneiss. Plane polarized **A** and cross polarized **B** photomicrographs of recrystallized elongate quartz and plagioclase crystals. The foliation is defined by the orientation of biotite and elongate minerals.

3.6 CHM09020A: Retrogressed eclogite, Utmarkamossen

This sample was taken from a garnet and clinopyroxene-rich mafic lens set in migmatitic gneisses.

3.6.1 Descriptions

This sample is made up of garnet, hornblende, quartz, plagioclase, clinopyroxene, and biotite with accessory phases of rutile and opaques. These minerals can be sorted into groups based on what mineral they form a pseudomorph of. Two different symplectites occur; a clinopyroxene, hornblende, plagioclase symplectite (cpx-symplectite) resulting from the break down of large clinopyroxene grains and a biotite, plagioclase symplectite (biotite-symplectite). Grain outlines of the clinopyroxene from which the cpx-symplectite has formed are still visible, and are 7-12 mm in length. The cpx-symplectite minerals have grown in a crosshatched 90° pattern and there is a very tight inter-

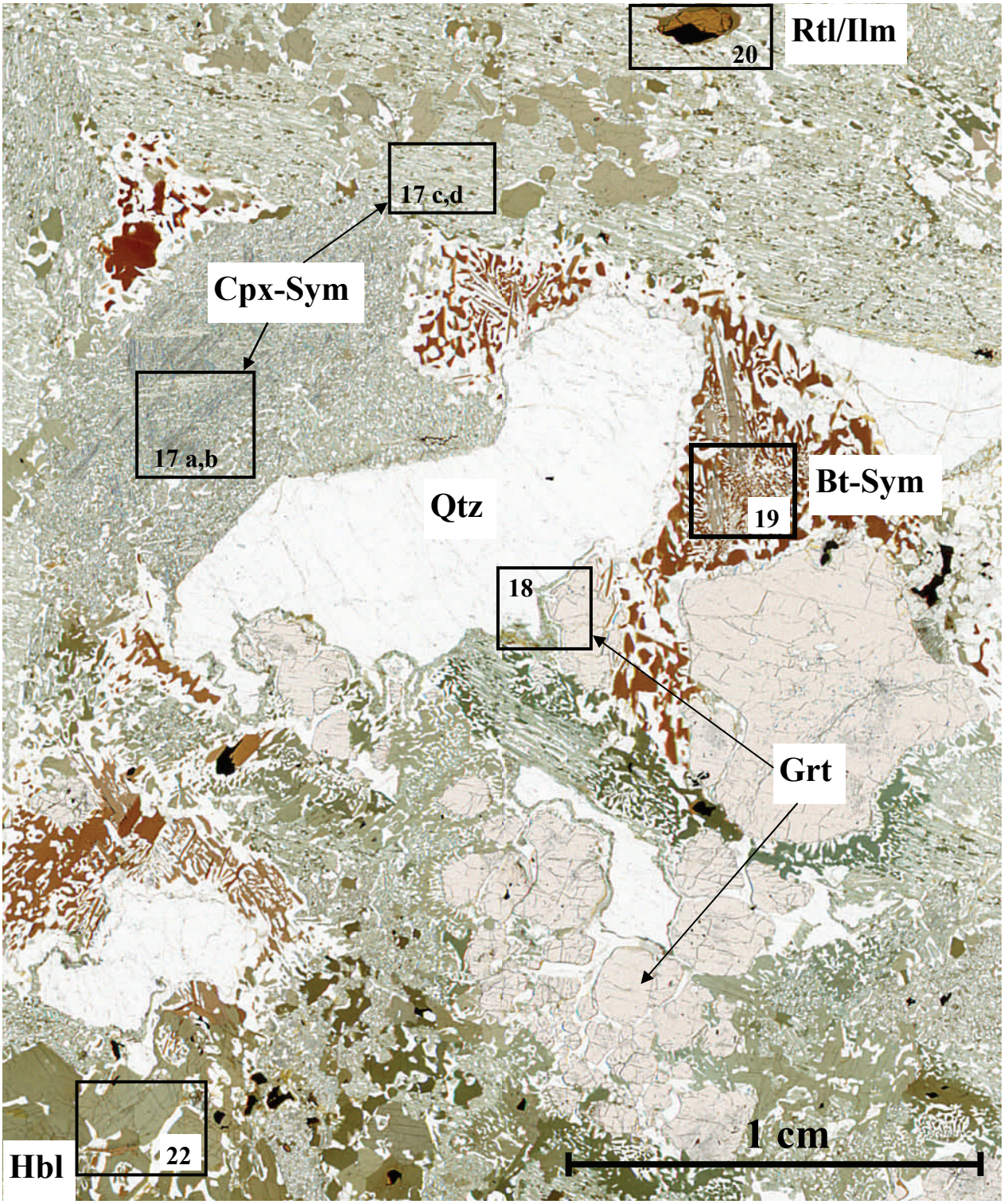

Figure 16. CHM09020A: Retrogressed eclogite. Scanned thin section showing pseudomorphs of large grains, and mineral relations and textures. Rtl/Ilm = rutile (brown) and ilmenite, Cpx-sym = clinopyroxen-symplectite, Bt-Sym = biotite-symplectite, qtz = quartz, Grt = garnet, Hbl = hornblende. Boxes denote locations where photos were taken.

growth of the clinopyroxene and hornblende (figure 17a,b). Other localities of the cpx-symplectite show an unlike parallel pattern, but remain the same chemically (figure 17c,d). In the areas where two large cpx-symplectite grains meet, there is an increase in the amount of plagioclase occurring as small rounded grains. Quartz exists as large 5-10 mm long euhedral crystals, with patchy undulose extinction. There is not a very prominent undulose extinction, the difference in extinction angles between the subgrains of quartz are ~8°. A corona texture around the quartz occurs near garnet. It consists of two phases, clinopyroxene nearest

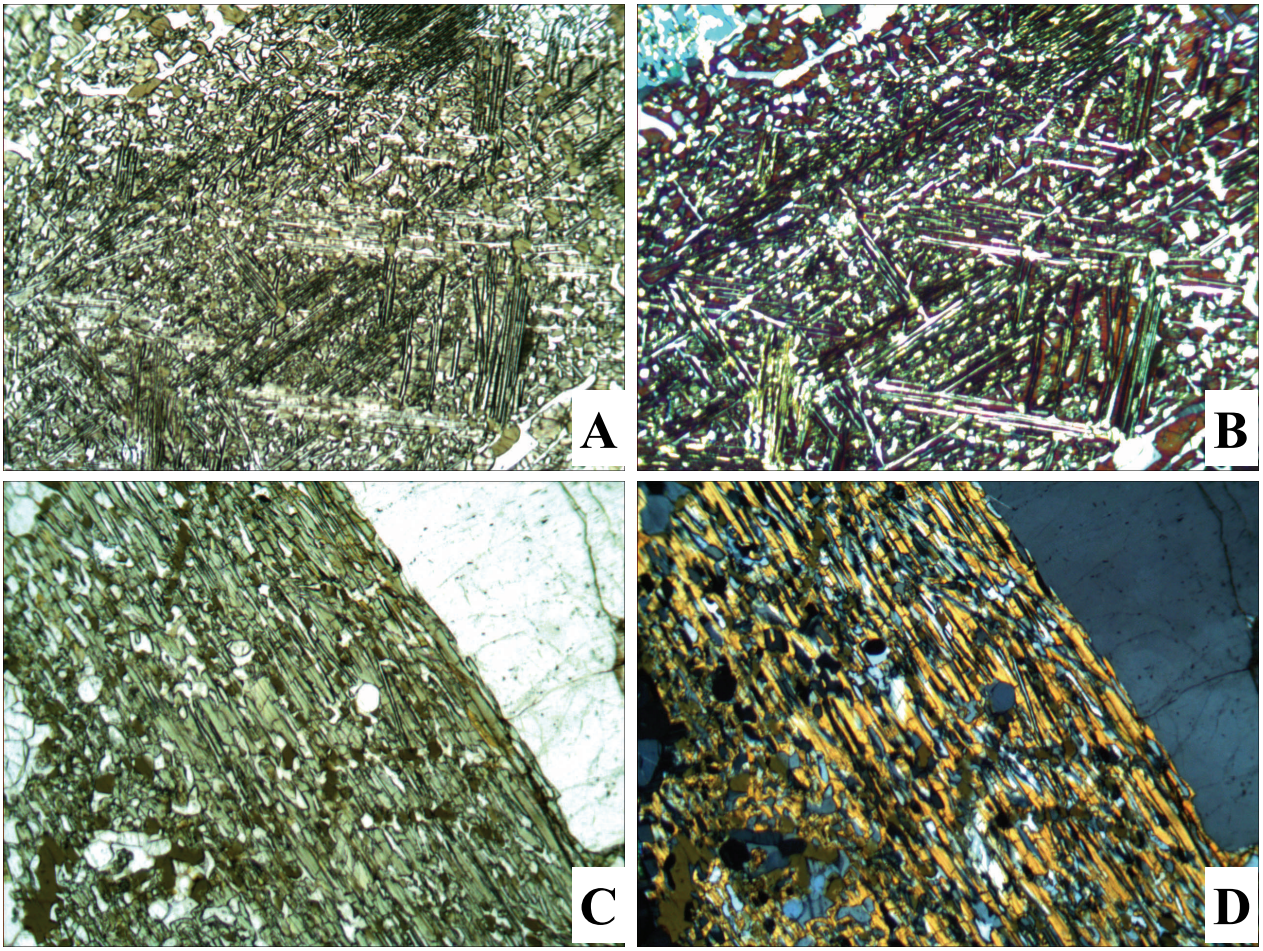

Figure 17. CHM09020A: Retrogressed eclogite. Photomicrograph of crosshatched cpx-symplectite, plane polarized **A** and crossed polarized **B**, parallel cpx-symplectite in contact with a quartz grain, plane polarized **C** and crossed polarized **D**.

quartz and plagioclase nearest garnet (figure 18). Garnet makes up approximately 25 percent of this section and it occurs as 3-6mm diameter crystals. The garnet crystals are mostly subhedral, but in some instances the garnet looks disaggregated and plagioclase and hornblende has grown between the grains. Inclusions of quartz and plagioclase with distinctly tapered twinning exist in the larger garnet grains. Hornblende also occurs as medium sized subhedral and anhedral crystals. Isolated grains are anhedral, but grains that form an aggregate of hornblende are subhedral. The biotite-symplectite is characterized by a vermicular intergrowth of biotite and plagioclase (figure 19). In the center of the largest biotite-symplectite present in this section there are multiple small quartz grains. A second phase of biotite has grown over part of the symplectite, and is distinguished by its different orientation showing the cleavage planes. Rutile exists in a few locations throughout the sample, everywhere in contact with an opaque phase. The largest rutile grain is located within a cpx-symplectite and there is a rim of hornblende surrounding the rutile crystal (figure 20).

3.6.2 SEM

A look at this section in the scanning electron microscope helped to confirm the composition of phases and also revealed some reaction sites which were previously unnoticed. There is a ~5µm wide reaction rim of amphibole which separates the clinopyroxene and plagioclase on the aforementioned garnet quartz reaction site. The opaque phase associated with rutile is ilmenite, which also occurs in smaller quantities scattered throughout the rock.

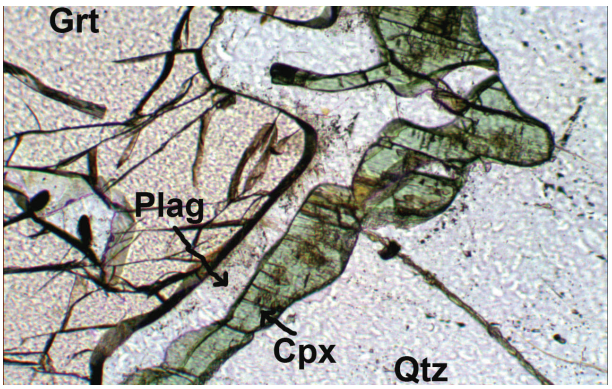

Figure 18. CHM09020A: Retrogressed eclogite. Photomicrograph under plane polarized light, clinopyroxene+plagioclase corona between garnet and quartz.

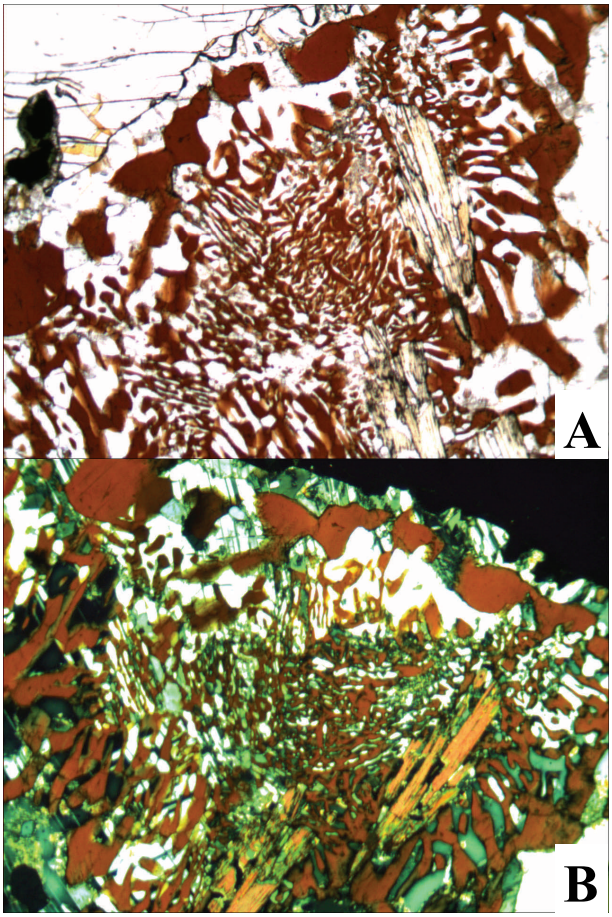

Figure 19. CHM09020A: Retrogressed eclogite. Photomicrograph under plane polarized **A** and cross polarized **B** light. Biotite-symplectite in contact with garnet (top left and right), note the second phase of

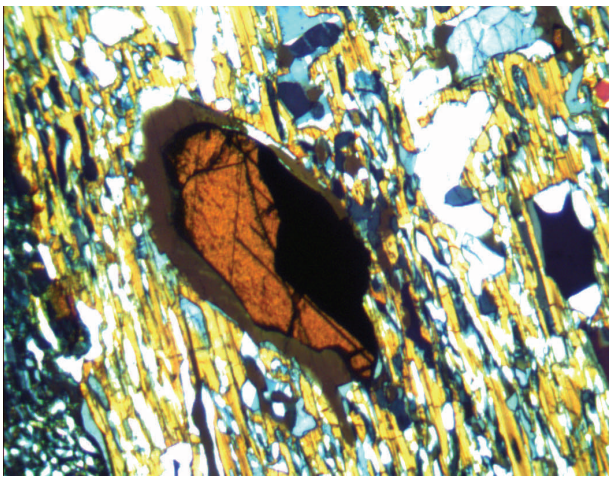

Figure 20. CHM09020A: Retrogressed eclogite. Rutile/ilmenite grain with hornblende rim inset in a parallel cpx-symplectite.

3.6.3 Interpretations

This rock is interpreted as a retro-eclogite. At one point in time large clinopyroxene, garnet and quartz grains dominated this rock, but retrogression occurred as lower pressure reactions replaced much of the clinopyroxene and dismembered the garnet. The cpx-symplectite resulted as a breakdown of the typical high-pressure phase omphacite, as described by Anderson and Moecher (2007). The different patterns seen in the cpx-symlectites may represent the original

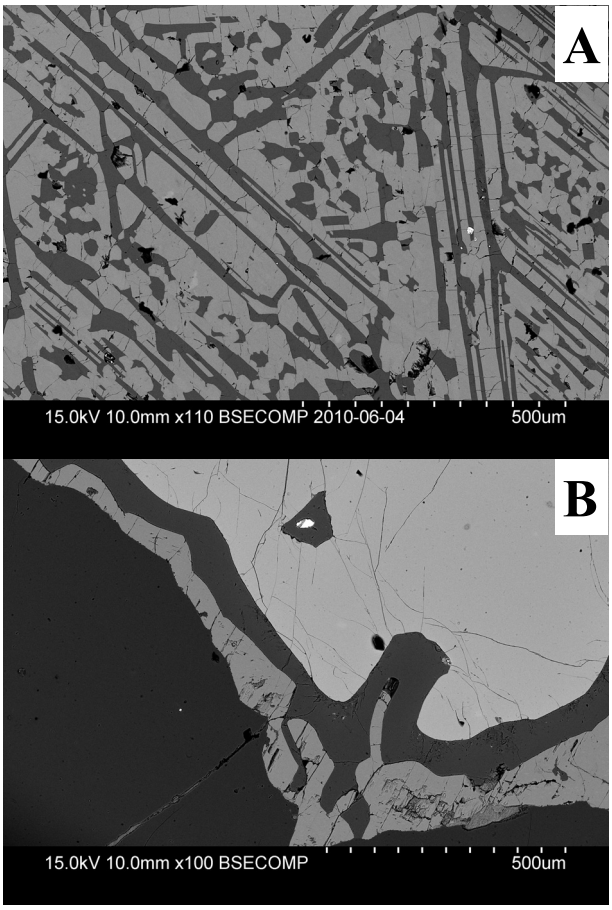

Figure 21. CHM09020A: Retrogressed eclogite. **A**) crosshatched cpx-symplectite, darker areas are plagioclase and lighter areas are hornblende and clinopyroxene, a difference in these two minerals is only noticed at very high contrast. **B**) clinopyroxene + plagioclase corona between garnet and quartz.

orientation of omphacite, as the exsolution processes are expected to follow mineral cleavage planes. The 'crosshatched' symplectite formed from an omphacite grain with a more equidimensional shape than the other grains, this may be explained by a different orientation of the crystal where this crystal is being viewed along the z-axis. The large hornblende crystals unassociated with the symplectites possibly formed at a later metamorphic event, their presence and apparent stability suggests retrogression took place under amphibolite facies conditions (figure 22). The textures suggest that plagioclase, although now occurring with nearly every phase was not present alongside garnet and omphacite. There are no plagioclase inclusions within the center of the largest garnet grain, and inclusions that do exist in smaller grains all exhibit metamorphic tapered twins. The spatial relation between

rutile and ilmenite could indicate a previous reaction between the phases, but no reaction textures were found so determining reaction kinetics is not possible. The amphibole rim around the rutile/ilmenite reacion sites could be explained by an increase in free Fe^{2+} released by the breakdown of ilmenite. The garnet, clinopyroxene, plagioclase, quartz reaction is a well-studied geobarometer common in retrogressed eclogites. Moecher et al (1988) as well as Anderson and Moecher (2007) review the various possible reaction paths these phases can take, but a simplified version is as follows;

garnet (grossular and pyrope) + quartz = clinopyroxene (diopside) + plagioclase (anorthite).

The origin of the biotite-symplectite is uncertain, but its formation under similar conditions as the cpx-symplectite is suggested. One inference that could be made suggests an origin stemming from a high-pressure phase with low stability in mid-pressure conditions. Wimmenauer and Stenger (1989) proposed a formation of biotite, plagioclase and spinel from the breakdown of phengite. Spinel has not been identified in this section; the reaction in the present retroeclogite may have been different due to the presence of free SiO_2.

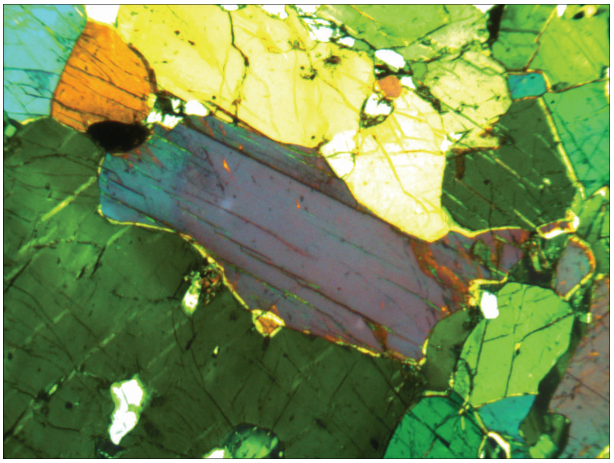

Figure 22. CHM09020A: Retrogressed eclogite. Photomicrograph taken under cross polarized light. Presumably late-stage hornblende aggregate (all colored grains seen in photo are hornblende)

3.7 CHM092020B: Grey migmatitic gneiss, Utmarkamossen

3.7.1 Descriptions

Foliations are unrecognizable on the thin-section scale, but the mafic constituents tend to form as mineral aggregates. Plagioclase makes up ~ 45 percent of the sample, and quartz accounts for another ~20 percent. The plagioclase and quartz occur mostly as similar sized rounded grains, which produce a granoblastic texture with well-formed triple junctions (figure 25). Garnet appearing as small cracked grains is scattered throughout the sample with no preferred orientation or grouping. Euhedral biotite and partly altered biotite account for ~10 percent of the rock (figure 24). Hornblende represents ~15 percent of the section; it is anhedral-subhedral and spatially associated with scapolite grains.

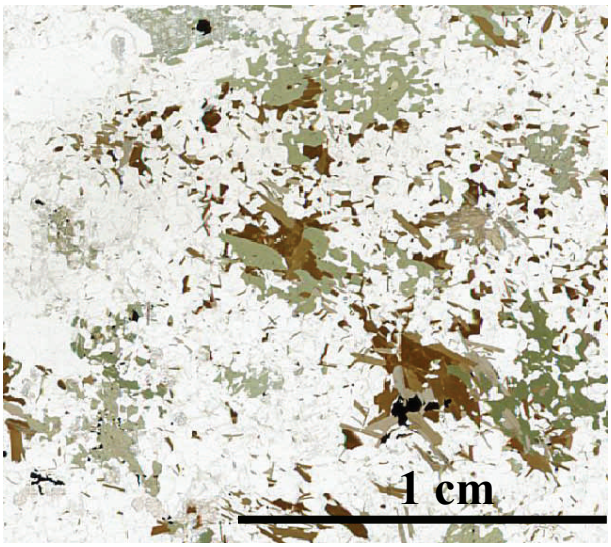

Figure 23. CHM092020B: Grey migmatitic gneiss. Cropped segment from scanned thin section showing mineral assemblages and the general texture.

3.7.2 Interpretations

This rock has had a similar metamorphic history as the previously discussed gneisses. The first recorded metamorphic event was one that took place at garnet-amphibolite conditions. Heating responsible for the granoblastic texture in the quartz and plagioclase took place during upper-amphibolites facies metamorphism accompanied by partial melting. An increase in heat is not needed for the rock to undergo recrystallization if the pressure is reduced faster than the heat is decreased. The most recent metamorphic episode was one, which occurred under low-pressure conditions, and is responsible for the alteration of biotite. The presence of scapolite suggests CO_2 and/or Cl rich fluids penetrated the rock.

Figure 24. CHM092020B: Grey migmatitic gneiss. Fibrous alteration of biotite under plane polarized light.

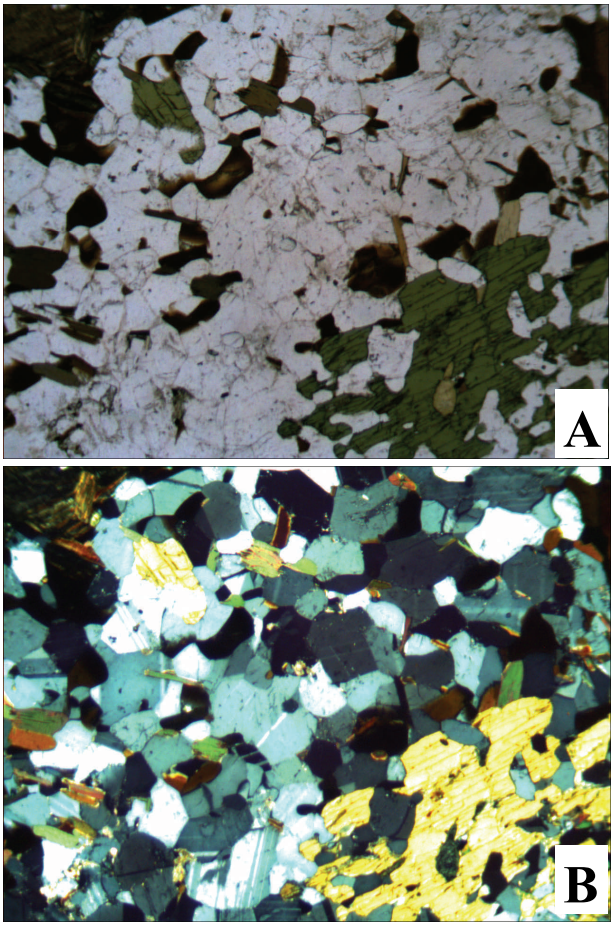

Figure 25. CHM092020B:Grey migmatitic gneiss. Plane polar **A**) and crossed polar **B**) photomicrographs showing granoblastic texture in quartz and plagioclase. Biotite is scattered throughout sample, anhedral hornblende in bottom right.

3.8 CHM092028A: Strongly deformed migmatitic gneiss, Skällstorp

3.8.1 Descriptions

Due to a high degree of recrystallization foliations are only recognized in biotite crystals and occasional ribbon shaped quartz. The parallelism of biotite varies by ~10°, and in some grains there is an intergrowth with muscovite. There is no hornblende identified in this section, and garnet appears sparsely as less than 1mm grains. Microcline and quartz make up ~85 percent of the rock; plagioclase is a minor phase. The feldspar and quartz grains, although nearly equal in size, do not produce a granoblastic texture; instead the grain boundaries are irregular and serrated.

3.8.2 Interpretations

Much of the strain in this rock has been accommodated by the recrystallization of feldspars and quartz. The highest pressure metamorphic grade visible this rock is controlled by the presence of garnet. A shearing event is responsible for the deformation and the alignment of biotite grains. The heating responsible for recrystallization is expected to have outlasted the deformation, since there are no indicators of syn-deformational recrystallization.

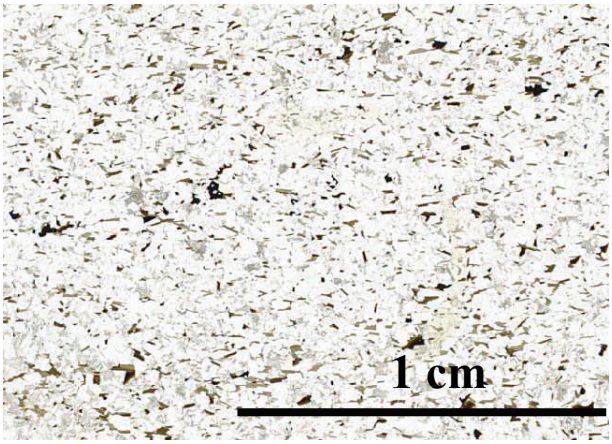

Figure 26. CHM092028A: Strongly deformed migmatitic gneiss. Cropped segment from scanned thin section showing mineral assemblages and the general texture.

Figure 27. CHM092028A: Strongly deformed migmatitic gneiss. Deformation is prominent at outcrop scale. Photo taken by Charlotte Möller.

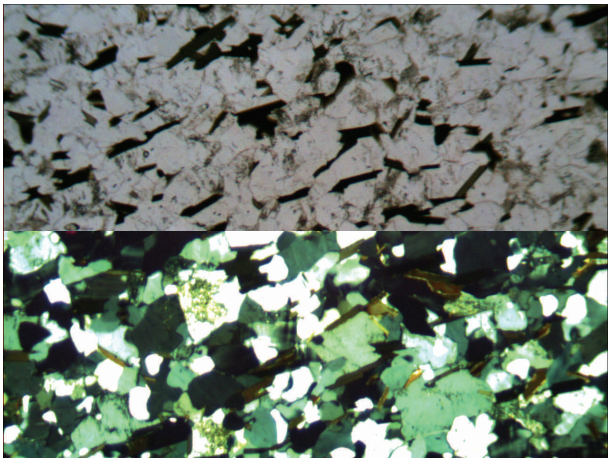

Figure 28. CHM092028A: Strongly deformed migmatitic gneiss. Plane polar (top) and crossed polars (bottom) photomicrograph. Note the alignment of biotite and the granoblastic texture exibited in the quartz and plagioclase.

3.9 CHM092029A: Strongly deformed gneiss, Skällstorp

3.9.1 Descriptions

Biotite and hornblende is present in the sample together with plagioclase, microcline, quartz leucosomes. Hornblende is subhedral and biotite is euhedral. The plagioclase shows signs of late stage alteration, possibly sericite. Plagioclase has tapered twins, and the feldspar and quarts crystals have irregular grain boundaries. Garnet is not present in this rock.

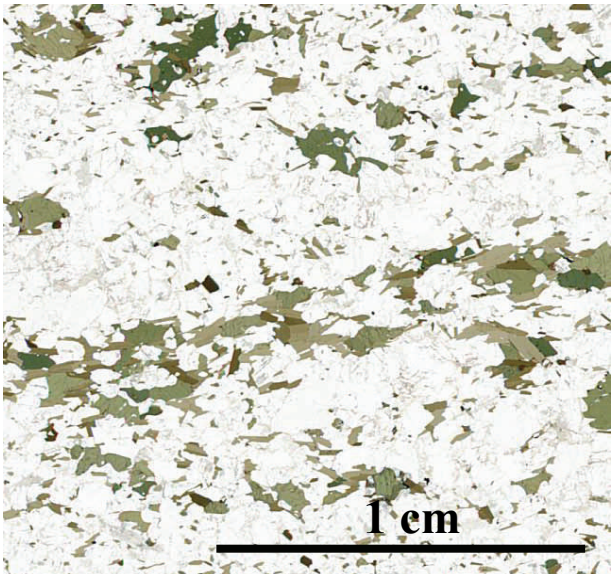

Figure 29. CHM092029A: Strongly deformed gneiss Cropped segment from scanned thin section showing mineral assemblages and the general texture.

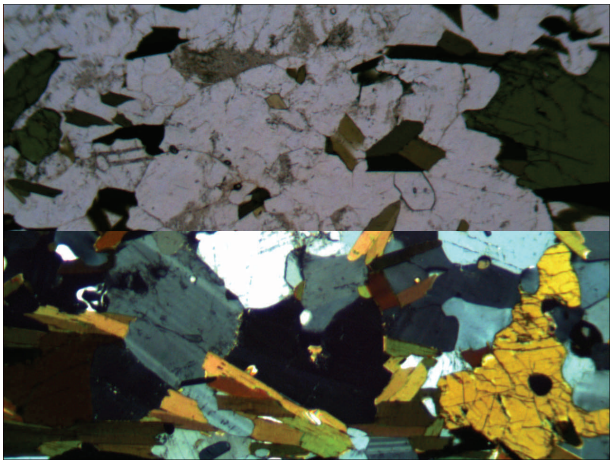

Figure 30. Strongly deformed gneiss.
Plane polar (top) and crossed polar (bottom) photomicrograph showing major minerals present in rock.

3.9.2 Interpretations

The lack of garnet is interesting (as it suggests this rock has not reached the same pressures as other nearby units have), although different rock composition and decomposing metamorphic reactions may be responsible for the absence of garnet. The gneissic foliations are quite well defined, and the presence of hornblende place the foliations as occurring in amphibolite facies conditions. The plagioclase is metamorphic in origin as determined by the occurrence of tapered twins, likely forming at the same time as the hornblende. Recrystallization has occurred, but as seen by the irregular grain boundaries and non-granoblastic texture it is far from completion.

3.10 CHM092029B: Migmatitic amphibolite, Skällstorp

3.10.1 Descriptions

Large 2-4 mm diameter garnets make up ~25 percent of this rock, and subhedral hornblende accounts for ~50 percent. The remaining 25 percent is made up of anhedral biotite, plagioclase and an opaque phase. The garnets are well formed and contain inclusions of quartz, hornblende and plagioclase. Plagioclase crystals exhibit tapered twins and some grains can be recognized as being mechanically bent. Hornblende grains have a unique curved or undulating fracture pattern that is a site for exsolution or secondary crystal growth (figure 32). The fractures trend in a uniform pattern throughout the sample, and a dominant set of fractures in garnets also align in the same direction. The opaque phase looks to be in reaction with garnet; it appears to produce plagioclase at the expense of garnet whenever they are near (figure 33).

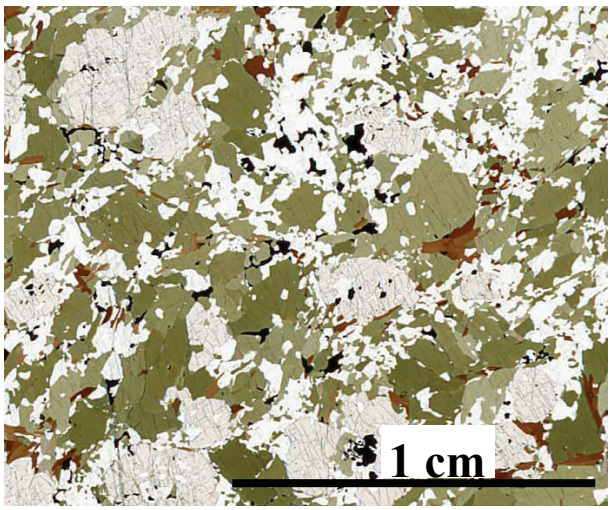

Figure 31. CHM092029B: Migmatitic amphibolite. Cropped segment from scanned thin section showing mineral assemblages and the general texture. Note the abundance of garnet and hornblende.

3.10.2 Interpretations

The garnet, hornblende and plagioclase all look to have grown at the same time, and the garnet amphibolite facies conditions are consistent with other samples studied. Tapered twins in plagioclase crystals indicate a metamorphic origin. This rock does not have as much quartz and plagioclase as the other nearby units, fracturing of the garnet and hornblende grains may be one way the rock has accommodated stress. Growth of plagioclase surrounding the opaques is expected to have happened some time after peak metamorphism,

possibly during a lower pressure metamorphic event. The timing of the deformation event in relation to metamorphic crystal growth and a possible heating event is uncertain and would require a more in depth analysis of the fracturing patterns and chemistry of the phases growing within the fractures.

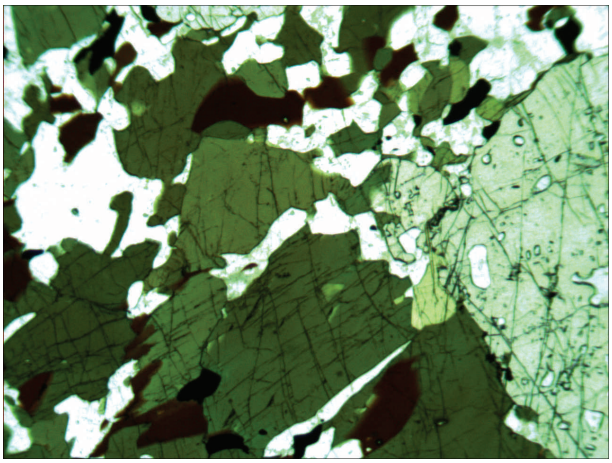

Figure 32. CHM092029B: Migmatitic amphibolite. Photomicrograph under plane polarized light. Hornblende exhibiting similarly trending curved fractures.

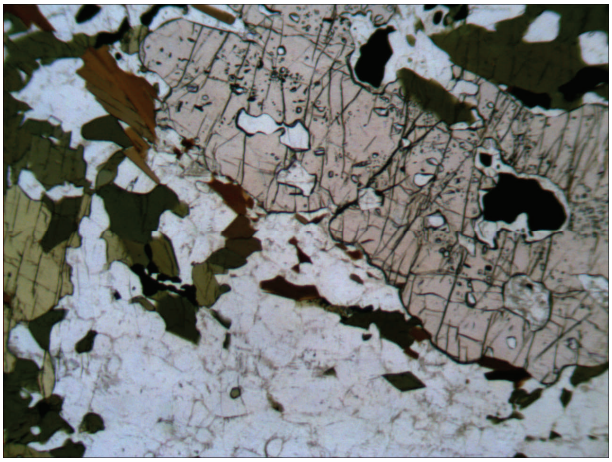

Figure 33. CHM092029B: Migmatitic amphibolite. Plane polarized photomicrograph of garnet grain with ilmenite inclusion, dominant fracture set align with the hornblende fracture pattern.

3.11 CHM092031A: Strongly deformed gneiss, Gällared

3.11.1 Field observations

This unit is a highly strained granitic gneiss with distinct gneissic banding. Multiple dolorite and pegmatite dykes cross-cut the outcrop. Foliation refraction is recognizable across the dykes due to competence contrasts (figure 34).

3.11.2 Descriptions

Two differing compositions of felsic bands are present, one type is nearly all quartz, whereas the other is ~75 percent plagioclase and microcline and ~25 percent quartz. Mafic microdomains are made up of hornblende and biotite. Hornblende is subhedral-anhedral and biotite is subhedral. There are a few garnet grains, all of which are quite small, fractured and resorbed. The plagioclase exhibits tapered twins. Quartz rich bands are granoblastic and show no signs of strain, the plagioclase variety is not nearly as recrystallized and still shows evidence of growth under stress, such as bent grains.

Figure 34. CHM092031A: Strongly deformed gneiss. Cut by a pegmatite. Note the difference in orientation of the foliation in the pegmatite versus the gneiss, indicating the high competence of the pegmatite.

Figure 35. CHM092031A: Strongly deformed gneiss. Cropped segment from scanned thin section showing mineral assemblages and the general texture.

3.11.3 Interpretations

This rock has been highly strained, and variable degrees of recovery have taken place throughout. The duration and temperature of crystal recovery can be approximated by the differences between the two types of felsic bands. There was enough heat and time for quartz grains to recover but not quite enough for the stronger feldspar rich bands to fully recover. The peak metamorphic degree recorded is upper-amphibolites facies. This sample exhibits evidence of a similar polymetamorphic history seen in the other samples of this study area; a formation of garnet followed by a lower pressure event where garnet becomes unstable and low-pressure alteration of biotite and plagioclase occurs.

3.12 Summary and interpretation of petrography

The samples can be sorted into two groups, mafic and felsic. The mafic rocks are the amphibolites, whereas the felsic rocks are all the varieties of gneisses. The retro-eclogite (sample 9020A) although mafic, will be addressed separately due to its petrological dissimilarities .

The main minerals common to all the felsic samples are: quartz, plagioclase and microcline with minor amounts of biotite and hornblende. A small amount of garnet is present in some of the felsic rocks, and it often looks resorbed. A late low grade alteration forming pumpellyite from biotite as well as sericite growth in plagioclase and microcline is visible in some of the samples. Various stages of crystal recovery occur in the samples. The less deformed rocks such as 2020B exhibit a more granoblastic texture with equidimensional crystals. Crystal recovery in the form of recrystallization and annealing in the strongly deformed gneisses produced elongate quartz grains. Metamorphic twinning in plagioclase is more prevalent in the rocks that appear to have undergone a lesser degree of annealing. Pinning and dragging structures are evidence for dynamic recrystallization; it shows the individual crystals are ductile when they are deformed. The highest pressure/temperature mineral found in the gneisses is garnet, but since it appears unstable it is not representative of the current metamorphic facies of the felsic rocks. Based on the presence and stability of hornblende in all the samples, the gneisses last equilibrated under amphibolite facies conditions.

The main minerals common to all the mafic samples are: hornblende, garnet, plagioclase and clinopyroxene. Minor amounts of biotite, quartz, microcline, and an opaque phase occur in the amphibolites. The presence of garnet and clinopyroxene in equilibrium with hornblende place the mafic samples in the upper amphibolites facies. The mafic rocks are more competent at higher temperatures, so the signs of strain and deformation seen in the felsic rocks are not commonly seen in the amphibolites. Microdomains that are feldspar and quartz rich show signs of recovery similar to what is seen in the gneisses. Late low grade alteration of biotite to pumpellyite and plagioclase to sericite happens to some extent in all the mafic rocks.

Retro-eclogite: This rock as been termed a retrogressed eclogite because, based on the textures and mineral assemblages especially the symplectites, it has been interpreted to have been mainly clinopyroxene (omphacite), garnet and quartz. There are no indications that plagioclase was part of the omphacite garnet assemblage, this indicates that the rock surpassed the upper stability limit of plagioclase (Figure 36; Borghini et al, 2010). The reaction between garnet and quartz in the retro-eclogite is a common decompression reaction:

Pyrope + grossular + quartz = diopside + anorthite

Rutile (TiO_2) is expected to be stable during eclogite facies, as is ilmenite ($FeTiO_3$). Korneliussen et al, (1999) showed that rutile will form from ilmenite at higher pressures if the rock composition is correct, this may have happened in this sample.

The precise cpx-symplectite formation reaction is unknown since chemistry of the symplectite was not studied. The symplectite resulted from the breakdown of omphacite, and began growing when the rock was

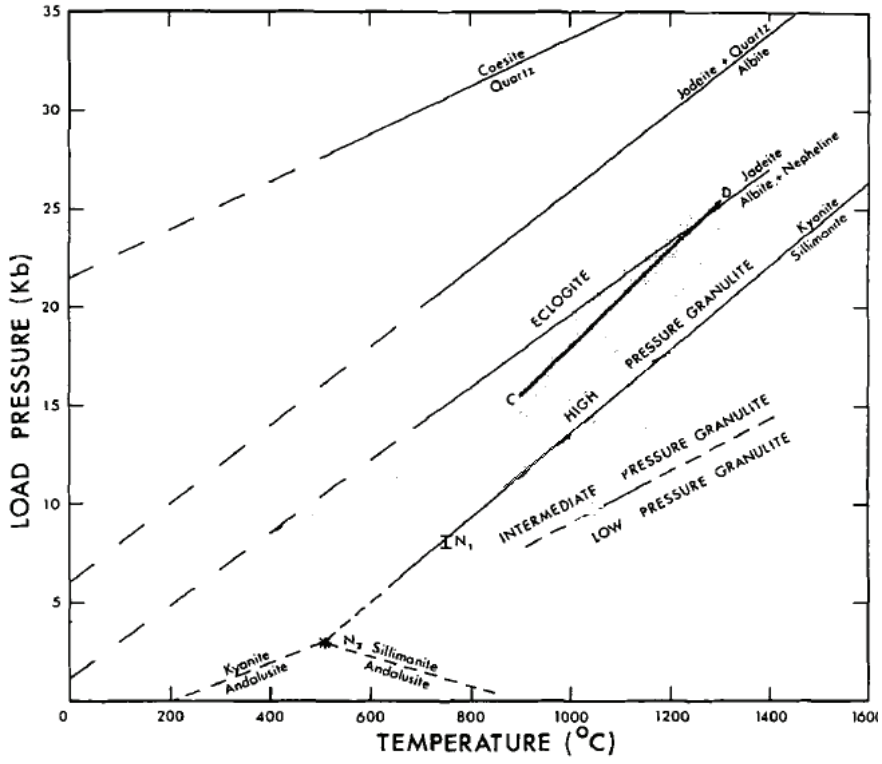

Figure 36. *P-T* diagram showing high pressure and temperature phase stability. Kyanite-silimanite-andalusite stability field included for reference. Line CD marks the disappearance of plagioclase in quartz tholeiite compositions. Figure modified from Green and Ringwood, (1967).

entered a pressure temperature range of about ~13kbar and 700°C (Anderson and Moecher, 2007). The reaction is expected to have stopped when the temperature was too low for diffusion to occur between the products.

The origin of the biotite-symplectite is uncertain, similar symplectites have been described and attributed to the breakdown of phengite (Groppo et al, 2007). Palmeri et al, (2003) describe a similar biotite-symplectite, and propose a phengite breakdown reaction which produces $K + H_2O$:

Phengite + quartz + Na + Ca + Fe = biotite + plagioclase + $K + H_20$

Chlorine and CO_2 rich fluids are interpreted to have been present in five of the ten samples studied by the occurrence of scapolite, and the scapolite appears to have grown during the amphibolite facies metamorphism. Samples from the Kilahed are outside the UDZ yet still bare scapolite, indicating similar metamorphic fluids affected units within and outside the UDZ. One explanation is the UDZ was near the same depth as the rocks sampled from the Kilahed location during amphibolization. Future studies may be able to use the presence of scapolite as an indicator for studying the degree of chlorine and CO_2 rich fluid penetration during metamorphism.

4 Tectonic context: a discussion

One interpretation of the samples and locations studied in this sample is as follows:

The eclogites within the UDZ are *in situ*, meaning the entire gneiss package within the UDZ was subjected to high pressure metamorphic conditions, this interpretation is based on the presence of garnet in nearly all samples and the assumption that all rocks were once subjected to higher pressures where garnet was stable. The mafic rocks also contain clinopyroxene which is a phase commonly associated with high-pressure assemblages. The 680-800°C and 8-12kbar upper-amphibolite condition reported by Johansson et al, (1991) and Wang & Lindh (1996), produced a strong overprint that masks most previous metamorphic assemblages, further complicating the metamorphic history. If the eclogites are *in situ* then the majority of eclogite facies rocks have retrogressed. Rubie, (1998) showed that during polyphase reactions, metastable phases can exist far from equilibrium for large amounts of time because stable phases are unable to nucleate. The larger the mafic body, the more likely it is that it contains domains that have escaped reequilibration during amphibolites facies deformation and fluid infiltration. The best-preserved eclogite reported so far from the UDZ is a 2x1 km mafic lens-shaped body situated at Lilla Ammås (Möller, 1998). Many smaller mafic bodies throughout the UDZ show no signs of previous eclogite equilibrium; this could be explained by complete retrogression under upper-amphibolite conditions when the rocks had been exhumed to a mid-crustal level. The increased deformation of the gneisses surrounding the eclogites may be explained by competency contrasts. The mafic bodies are more competent than the more felsic gneisses protoliths, so strain that is not accomodated by deformation of the mafic bodies was accounted for in the surrounding gneisses. This is an outcrop and map scale process similar to how foliations deflect around garnet grains in garnet bearing mylonites. One criticism of this interpretation points to the presence of large mafic bodies that are completely granulitic or amphibolitic and smaller eclogite bodies. These mafic bodies may have experienced varying degrees of hydration by metamorphic fluids, which would increase the efficiency of re-equilibrium.

When viewed on a larger scale, the maximum age of eclogitisation in the Eastern Segment is 972 ± 14 Ma, during the Falkenberg phase (Johansson et al, 2001). Eclogitisation was followed by gravitational collapse in the Dalane phase (970-900 Ma), which is responsible for exhuming the rocks to mid-crustal levels (Bingen et al, 2008). Rather than a separate shearing event responsible for thrusting up high-pressure eclogite bodies into medium-pressure gneisses, there may be variable efficiency in the upper-amphibolite overprinting. High temperatures are required for the observed migmatization and recrystallization. If the eclogites are *in situ* then the whole UDZ would have been exhumed from the depths in excess of 50 km to mid-crustal levels, and the remnant heat associated with this decompression may be responsible for the high temperature textures.

5 Conclusion

Understanding what happened to the UDZ is a small yet important piece to figuring out the Sveconorwegian orogeny. This detailed microscopy study of the ten samples taken from within the Ullared Deformation Zone in southwest Sweden, has revealed information regarding the pressure-temperature evolution of the UDZ. Metamorphic conditions varied throughout the Sveconorwegian orogeny; the samples studied in this project show evidence for achieving (or nearly achieving) equilibrium in more than one metamorphic condition. The UDZ is interpreted to have been subjected to high-pressure granulite and eclogite conditions followed by a period in upper-amphibolite conditions. This is thought to be due to a rapid exhumation via tectonic stripping to mid-crustal levels followed by exhumation to the present day surface level. The decrease in pressure associated with this interpretation may be responsible for decompressive 'heating' of the UDZ gneisses which can be seen by the migmatization of some units and recrystallization of others. Further petrographic and structural studies of the UDZ and are needed to form a clearer picture of the Eastern Segments Sveconorwegian history.

Acknowledgements

I would like to thank Charlotte Möller for all the time she spent reviewing my results and giving me guidance. Her insights and discussions were invaluable. I would also like to thank my co-advisor Leif Johansson for his help with the microscopy and Anders Lindh for his instructions regarding the SEM.

6 References

Åhäll, K.I. & Larson, Å., 2000: Growth-related 1.85-1.55 Ga magmatism in the Baltic Shield: a review addressing the tectonic characteristics of Svecofennian, TIB 1 -related, and Gothian events. *GFF* 122, 193-206.

Anderson, E.D. & Moecher, D.P., 2007: Omphacite breakdown reactions and relation to eclogite exhumation rates. *Contributions to Mineral Petrology* 154, 253-277.

Andersson, J., Möller, C. & Johansson, L., 2002: Zircon chronology of migmatite gneisses along the Mylonite Zone (S Sweden): a major Sveconorwegian terrane boundary in the Baltic Shield. *Precambrian Research* 114, 121-147.

Andersson, J., Söderlund, U., Cornell, D., Johansson, L. & Möller, C., 1999: Sveconorwegian (-Grenvillian) deformation, metamorphism and leucosome formation in SW Sweden, SW Baltic Shield: constraints from a Mesoproterozoic granite intrusion. *Precambrian Research* 98, 151-171.

Andersson, M., Lie, J.E. & Husebye, E.S., 1996: Tectonic setting of postorogenic granites within SW Fennoscandia based on deep seismic and gravity data. *Terra Nova* 8, 558-566.

Austin Hegardt, E., Cornell, D.H., Claesson, L., Simakov, S., Stein, H.J. & Hannah, J.L., 2005: Eclogites in the central part of the Sveconorwegian Eastern Segment of the Baltic Shield: support for an extensive eclogite terrane. *GFF* 127, 221-232.

Bingen, B., Nordgulen, O. & Viola, G., 2008: A four-phase model for the Sveconorwegian orogeny, SW Scandinavia. *Norwegian Journal of Geology* 88, 43-72

Bingen, B., Skår, Ø., Marker, M., Sigmond, E.M.O., Nordgulen, Ø., Ragnhildstveit, J., Mansfeld, J., Tucker, R.D. & Liégeois, J.P., 2005: Timing of continental building in the Sveconorwegian orogen, SW Scandinavia. *Norwegian Journal of Geology* 85, 87-116.

Bingen, B. & van Breemen, O., 1998: Tectonic regimes and terrane boundaries in the high-grade Sveconorwegian belt of SW Norway, inferred from U–Pb zircon geochronology and geochemical signature of augen gneiss suites. *Journal of the Geological Society, London* 155, 143-154.

Borghini, G., Fumagalli, P. & Rampone, E., 2010: The stability of plagioclase in the upper mantle: subsolidus experiments on fertile and depleted lherzolite. *Journal of Petrology* 51, 229-254.

de Haas, G.J.L.M., Andersen, T. & Vestin, J., 1999: Detrital zircon geochronology: new evidence for an old model for accretion of the SW Baltic Shield. *Journal of Geology* 107, 569-586.

Green, D.H. & Ringwood, A.E., 1967: An experiment tal investigation of the gabbro to eclogite transformation and its petrological applications. *Geochimica et Cosmochimica Acta* 31, 767-833.

Groppo, C., Lombardo, B., Rolfo, F. & Pertusati, P., 2007: Clockwise exhumation path of granulitized eclogites from the Ama Drime range (Eastern Himalayas). *Journal of Metamorphic Geology* 25/1, 51-75

Hoffman, P.F., 1991: Did the breakout of Laurentia turn Gondwanaland inside-out? *Science* 252, 1409-1412.

Johansson, L., Lindh, A. & Möller, C., 1991: Late Sveconorwegian (Grenville) high-pressure granulite facies metamorphism in southwest Sweden. *Journal of Metamorphic Geology* 9, 283-292.

Johansson, L., Möller, C. & Söderlund, U., 2001: Geochronology of eclogite facies metamorphism in the Sveconorwegian Province of SW Sweden. *Precambrian Research* 106, 261-275.

Korneliussen, A., Erambert, M., McLimans, R. & Lloyd, F., 1999: Ti/Fe-Ti oxides at different metamorphic stages in the Sunnfjord region, W. Norway: Implications for the genesis of rutile (eclogite) ore deposits. *In*: Stanley, C.J. et al. (eds.) *Mineral Deposits: Processes to Processing.* Balkema, Rotterdam, 1105-1108.

Möller, C., 1999: Sapphirine in SW Sweden: a record of Sveconorwegian (-Grenvillian) late-orogenic tectonic exhumation. *Journal of Metamorphic Geology* 17, 127-141.

Möller, C., Andersson, J., Lundqvist, I. & Hellström, F.A., 2007: Linking deformation, migmatite formation and zircon U-Pb geochronology in polymetamorphic gneisses, Sveconorwegian province, Sweden. *Journal of Metamorphic Geology* 25, 727-750.

Möller, C., Andersson, J., Söderlund, U., & Johans son, L., 1997: A Sveconorwegian deformation zone (system?) within the Eastern Segment, Sveconorwegian orogen of SW Sweden- a first report. *GFF* 119, 73-78.

Möller, C. & Söderlund, U., 1997: Age constraints on the regional deformation within the Eastern Segment, S. Sweden: Late Sveconorwegian granite dyke intrusion and metamorphic deformational relations. *GFF* 119, 1-12.

Palmeri, R., Ghiribelli, B., Talarico, F. & Ricci, C.A.,

2003: Ultra-high-pressure metamorphism in felsic rocks: the garnet-phengite gneisses and quarzites from the Lanterman Range, Antarctica. *European Journal of Mineralogy* 15, 513-525.

Park, R.G., Åhäll, K.I. & Boland, M.P., 1991: The Sveconorwegian shear-zone network of SW Sweden in relation to mid-Proterozoic plate movements. *Precambrian Research* 49, 245-260.

Rubie, C.D., 1998: Disequilibrium during metamorphism: the role of nucleation kinetics. *Geological Society of London, Special Publications* 138, 199-214.

Söderlund, U., Hellström, F.A. & Kamo, S.L., 2008: Geochronology of high-pressure mafic granulite dykes in SW Sweden: tracking the P- T-t path of metamorphism using Hf isotopes in zircon and baddeleyite. *Journal of Metamorphic Geology* 26, 539-560.

Söderlund, U., Isachsen, C.E., Bylund, G., Heaman, L.M., Patchett, P.J., Vervoort, J.D. & Anders son, U.B., 2005: U-Pb baddeleyite ages, and Hf, Nd isotope chemistry constraining repeated mafic magmatism in the Fennoscandian Shield from 1.6 to 0.9 Ga. *Contributions to Mineral ogy and Petrology* 150, 174-194.

Söderlund, U., Möller, C., Andersson, J., Johansson, L. & Whitehouse, M.J., 2002: Zircon geochronology in polymetamorphic gneisses in the Sveconorwgian orogen, SW Sweden: ion microprobe evidence for 1.46-1.42 Ga and 0.98-0.96 Ga reworking. *Precambrian Research* 113, 193-225.

Söderlund, P., Söderlund, U., Möller, C., Gorbatschev, R. & Rodhe, A., 2004: Petrology and ion microprobe U-Pb chronology applied to a metabasic intrusion in southern Sweden: a study on zircon formation during metamorphism and deformation. *Tectonics* 23.

Tomkins, H.S., Williams, I.S. & Ellis, D.J., 2005: In situ U-Pb dating of zircon formed from retrograde garnet breakdown during decompression in Rogaland, SW Norway. *Journal of Metamorphic Geology* 23, 201-215.

Wahlgren, C.H., Cruden, A.R. & Stephens, M.B., 1994: Kinematics of a major fan-like structure in the eastern part of the Sveconorwegian orogen, Baltic Shield, south-central Sweden. *Precambrian Research* 70, 67-91.

Wang, X.D. & Lindh, A., 1996: Temperature-pressure investigation of the southern part of the Southwest Swedish Granulite Region. *European Journal of Mineralogy* 8, 51-67.

Tidigare skrifter i serien ”Examensarbeten i Geologi vid Lunds Universitet”:

219. Åkesson, Maria, 2008: Mud volcanoes - a review. (15 hskp)
220. Randsalu, Linda, 2008: Holocene relative sea-level changes in the Tasiusaq area, southern Greenland, with focus on the Ta1 and Ta3 basins. (30 hskp)
221. Fredh, Daniel, 2008: Holocene relative sea-level changes in the Tasiusaq area, southern Greenland, with focus on the Ta4 basin. (30 hskp)
222. Anjar, Johanna, 2008: A sedimentological and stratigraphical study of Weichselian sediments in the Tvärkroken gravel pit, Idre, west-central Sweden. (30 hskp)
223. Stefanowicz, Sissa, 2008: Palyno-stratigraphy and palaeoclimatic analysis of the Lower - Middle Jurassic (Pliens-bachian - Bathonian) of the Inner Hebrides, NW Scotland. (15 hskp)
224. Holm, Sanna, 2008: Variations in impactor flux to the Moon and Earth after 3.85 Ga. (15 hskp)
225. Bjärnborg, Karolina, 2008: Internal structures in detrital zircons from Hamrånge: a study of cathodolumine-scence and back-scattered electron images. (15 hskp)
226. Noresten, Barbro, 2008: A reconstruction of subglacial processes based on a classification of erosional forms at Ramsvikslandet, SW Sweden. (30 hskp)
227. Mehlqvist, Kristina, 2008: En mellanjuras-sisk flora från Bagå-formationen, Bornholm. (15 hskp)
228. Lindvall, Hanna, 2008: Kortvariga effekter av tefranedfall i lakustrin och terrestrisk miljö. (15 hskp)
229. Löfroth, Elin, 2008: Are solar activity and cosmic rays important factors behind climate change? (15 hskp)
230. Damberg, Lisa, 2008: Pyrit som källa för spårämnen – kalkstenar från övre och mellersta Danien, Skåne. (15 hskp)
331. Cegrell, Miriam & Mårtensson, Jimmy, 2008: Resistivity and IP measurements at the Bolmen Tunnel and Ådalsbanan, Sweden. (30 hskp)
232. Vang, Ina, 2008: Skarn minerals and geological structures at Kalkheia, Kristiansand, southern Norway. (15 hskp)
233. Arvidsson, Kristina, 2008: Vegetationen i Skandinavien under Eem och Weichsel samt fallstudie i submoräna organiska avlagringar från Nybygget, Småland. (15 hskp)
234. Persson, Jonas, 2008: An environmental magnetic study of a marine sediment core from Disko Bugt, West Greenland: implications for ocean current variability. (30 hskp)
235. Holm, Sanna, 2008: Titanium- and chromium-rich opaque minerals in condensed sediments: chondritic, lunar and terrestrial origins. (30 hskp)
236. Bohlin, Erik & Landen, Ludvig, 2008: Geofysiska mätmetoder för prospektering till ballastmaterial. (30 hskp)
237. Brodén, Olof, 2008: Primär och sekundär migration av hydrokarboner. (15 hskp)
238. Bergman, Bo, 2009: Geofysiska analyser (stångslingram, CVES och IP) av lagerföljd och lakvattenrörelser vid Albäcksdeponin, Trelleborg. (30 hskp)
239. Mehlqvist, Kristina, 2009: The spore record of early land plants from upper Silurian strata in Klinta 1 well, Skåne, Sweden. (45 hskp)
239. Mehlqvist, Kristina, 2009: The spore record of early land plants from upper Silurian strata in Klinta 1 well, Skåne, Sweden. (45 hskp)
240. Bjärnborg, Karolina, 2009: The copper sulphide mineralization of the Zinkgruvan deposit, Bergslagen, Sweden. (45 hskp)
241. Stenberg, Li, 2009: Historiska kartor som hjälp vid jordartsgeologisk kartering – en pilotstudie från Vångs by i Blekinge. (15 hskp)
242. Nilsson, Mimmi, 2009: Robust U-Pb baddeleyite ages of mafic dykes and intrusions in southern West Greenland: constraints on the coherency of crustal blocks of the North Atlantic Craton. (30 hskp)
243. Hult, Elin, 2009: Oligocene to middle Miocene sediments from ODP leg 159, site 959 offshore Ivory Coast, equatorial West Africa. (15 hskp)
244. Olsson, Håkan, 2009: Climate archives and the Late Ordovician Boda Event. (15 hskp)
245. Wollein Waldetoft, Kristofer, 2009: Svekofennisk granit från olika metamorfa miljöer.

(15 hskp)

246. Månsby, Urban, 2009: Late Cretaceous coprolites from the Kristianstad Basin, southern Sweden. (15 hskp)
247. MacGimpsey, I., 2008: Petroleum Geology of the Barents Sea. (15 hskp)
248. Jäckel, O., 2009: Comparison between two sediment X-ray Fluorescence records of the Late Holocene from Disko Bugt, West Greenland; Paleoclimatic and methodological implications. (45 hskp)
249. Andersen, Christine, 2009: The mineral composition of the Burkland Cu-sulphide deposit at Zinkgruvan, Sweden – a supplementary study. (15 hskp)
250. Riebe, My, 2009: Spinel group minerals in carbonaceous and ordinary chondrites. (15 hskp)
251. Nilsson, Filip, 2009: Föroreningsspridning och geologi vid Filborna i Helsingborg. (30 hskp)
252. Peetz, Romina, 2009: A geochemical characterization of the lower part of the Miocene shield-building lavas on Gran Canaria. (45 hskp)
253. Åkesson, Maria, 2010: Mass movements as contamination carriers in surface water systems – Swedish experiences and risks.
254. Löfroth, Elin, 2010: A Greenland ice core perspective on the dating of the Late Bronze Age Santorini eruption. (45 hskp)
255. Ellingsgaard, Óluva, 2009: Formation Evaluation of Interlava Volcaniclastic Rocks from the Faroe Islands and the Faroe-Shetland Basin. (45 hskp)
256. Arvidsson, Kristina, 2010: Geophysical and hydrogeological survey in a part of the Nhandugue River valley, Gorongosa National Park, Mozambique. (45 hskp)
257. Gren, Johan, 2010: Osteo-histology of Mesozoic marine tetrapods – implications for longevity, growth strategies and growth rates. (15 hskp)
258. Syversen, Fredrikke, 2010: Late Jurassic deposits in the Troll field. (15 hskp)
259. Andersson, Pontus, 2010: Hydrogeological investigation for the PEGASUS project, southern Skåne, Sweden. (30 hskp)
260. Noor, Amir, 2010: Upper Ordovician through lowermost Silurian stratigraphy and facies of the Borenshult-1 core, Östergötland, Sweden. (45 hskp)
261. Lewerentz, Alexander, 2010: On the occurrence of baddeleyite in zircon in silica-saturated rocks. (15 hskp)
262. Eriksson, Magnus, 2010: The Ordovician Orthoceratite Limestone and the Blommiga Bladet hardground complex at Horns Udde, Öland. (15 hskp)
263. Lindskog, Anders, 2010: From red to grey and back again: A detailed study of the lower Kundan (Middle Ordovician) 'Täljsten' interval and its enclosing strata in Västergötland, Sweden. (15 hskp)
264. Rääf, Rebecka, 2010: Changes in beyrichiid ostracode faunas during the Late Silurian Lau Event on Gotland, Sweden. (30 hskp)
265. Petersson, Andreas, 2010: Zircon U-Pb, Hf and O isotope constraints on the growth versus recycling of continental crust in the Grenville orogen, Ohio, USA. (45 hskp)
266. Stenberg, Li, 2010: Geophysical and hydrogeological survey in a part of the Nhandugue River valley, Gorongosa National Park, Mozambique – Area 1 and 2. (45 hskp)
267. Andersen, Christine, 2010: Controls of seafloor depth on hydrothermal vent temperatures - prediction, observation & 2D finite element modeling. (45 hskp)
268. März, Nadine, 2010: When did the Kalahari craton form? Constraints from baddeleyite U-Pb geochronology and geo-chemistry of mafic intrusions in the Kaapvaal and Zimbabwe cratons. (45 hskp)
269. Dyck, Brendan, 2010: Metamorphic rocks in a section across a Svecnorwegian eclogite-bearing deformation zone in Halland: characteristics and regional context. (15 hskp)

LUNDS UNIVERSITET

Geologiska enheten
Institutionen för geo- och ekosystemvetenskaper
Sölvegatan 12, 223 62 Lund